SUPPORTING INFORMATION

Supporting Information

Spin Me Right Round – A Versatile BTA-Based Alignment Media Toolbox for Enhanced Enantiodiscrimination

Matthias Brauser, Martin Leyendecker, Volker Schmidts, Christina M. Thiele*

SUPPORTING INFORMATION

Table of Contents

SUPPORTING INFORMATION

S1. General Information

S1.1 Chemicals used

The analytes (+)-β-pinene (+)-**1** and (-)-β-pinene (−)-**1** were purchased from Sigma-Aldrich and used as received. (*S*)-Octan-2-amine **12** was purchased from Sigma-Aldrich and used as delivered. $CDCl_3$ was purchased from Sigma-Aldrich and distilled over CaH_2 before use in the nuclear magnetic resonance spectroscopy (NMR) samples. Synthesis of the Sergeant and Soldier (SaS) BTAs (N^1,N^3,N^5-tri-n-dodecylbenzene-1,3,5-tricarboxamide **4**, N^1,N^3,N^5-tri((*R*)-Octan-2-yl)benzene-1,3,5-tricarboxamide (*R*)**-3** and N^1,N^3,N^5-tri((*S*)-Octan-2-yl)benzene-1,3,5-tricarboxamide (*S*)**-3** was carried out following the procedure published previously[1]. Synthesis of the asymmetrically substituted BTAs (*R*)-N^1,N^3-didodecyl-N^5-(Octan-2-yl)benzene-1,3,5-tricarboxamide (*R*)**-2** and (*S*)-N^1,N^3-didodecyl-N^5-(Octan-2-yl)benzene-1,3,5-tricarboxamide (*S*)**-2** and their precursors methyl-3,5-bis(dodecylcarbamoyl)benzoate **9** and 3,5-bis(dodecylcarbamoyl)benzoic acid **10** was carried out according to the experimental procedures described in section S4. Additional ^{1}H- and ^{13}C-NMR spectra of all compounds synthesized for this work are found in section S4 as well as high-resolution mass spectrometry spectra (HRMS) (where applicable) using the electrospray ionization (ESI) or the atmospheric pressure chemical ionization (APCI) method.

S2. NMR

S2.1 Instrumental equipment

NMR spectra to characterize the products synthesized were recorded on a Bruker Avance III system with 600 MHz proton frequency, equipped with a 5 mm triple-resonance broadband inverse probe (^{1}H, ^{2}H, ^{31} P, BB) or a Bruker Avance III HD 700 MHz spectrometer with a 5 mm quadruple resonance inverse cryoprobe (^{1}H/^{19}F,^{13}C, ^{31}P, ^{15}N) equipped with a z-gradient coil or a 400 MHz Bruker AVANCE III HD with BBFO probe. All anisotropic measurements were conducted on the 600 MHz Bruker Avance III system.

S2.2 Anisotropic NMR sample preparation

The anisotropic NMR samples (see Table S2.4 for composition) for the Sergeant-and-Soldier (SaS) BTA experiments were prepared by dissolving BTAs (**4** and (*R*)**-3** or (*S*)**-3**) as well as (+)-**1** or (−)-**1** in $CDCl_3$ in a 5 mm NMR tube. To avoid strong interference in the self-association process of the BTAs, instead of centrifugation or an ultra-sonic treatment, the samples were homogenized by repeatedly turning the NMR tube upside down. Before NMR measurements the samples were placed in the NMR magnet for equilibration periods of 30 to 60 minutes until a constant quadrupolar splitting and linewidth is observed. The homogeneity of the samples was inspected by ^{2}H-NMR images.[2] The same procedure is followed for the asymmetrically substituted BTAs (see Table S2) where BTA ((*R*)**-2** or (*S*)**-2**) is dissolved in $CDCl_3$ in a 5 mm NMR tube. To all anisotropic samples a DMSO-d_6 capillary is added to ensure an isotropic lock signal before they were flame sealed.

S2.3 Experimental parameters

Perfect-CLIP-HSQC[3] spectra: Perfect-CLIP-HSQC spectra were recorded with a total of 8192 data points (1.0 s acquisition time) in F2 and 512 data points (17 ms acquisition time) in F1 (NS = 8, DS = 8). For processing, the data was zero filled to 16384 points in F2 and 1024 points in F1.

2D TSE-PSYCHEDELIC[4] spectra: 2D TSE-PSYCHEDELIC spectra were recorded with 8192 data points (820 ms acquisition time) in F2 and 128 data points (1.3 s acquisition time) in F1 resulting in an FID resolution of 0.78 Hz in F1 (NS=32, DS=16). Selective refocusing was achieved using *RSnob*[5] 180° pulses with optimized bandwidths (see section S2.5 for more information). The offset was set according to the desired proton's resonance frequency. Zero filling was applied to 32768 data points in F2 and 512 points in F1.

CT-β-COSY[4b] spectra: CT-β-COSY spectra were recorded with 8192 data points resulting in a FID resolution of about 0.73 Hz in F2 and 256 data points resulting in a FID resolution of about 23 Hz in F1 (NS=16, DS=32). A factor of 2.5 was used for the scaling of *J*. Selective refocusing was achieved using *RSnob*[5] 180° pulses as described for the PSYCHEDELIC experiment above. The offset was set according to the desired protons resonance frequency. For processing, the data was zero filled to 16384 points in F2 and 1024 points in F1.

P.E.HSQMBC[6] spectra: P.E.HSQMBC spectra were recorded with 4096 data points (570 ms acquisition time) in F2 and 128 data points (4 ms acquisition time) in F1 (NS=32, DS=32). The INEPT delay was optimized for a long-range coupling constant ($^nJ_{CH}$) of 7

Hz. The delay in the G-BIRD element was optimized for a coupling constant ($^1J_{CH}$) of 145 Hz. A factor of 5 was used for $^1J_{CH}$-scaling. Selective refocusing during INEPT was achieved using *RSnob*[5] 180° pulses. The offset was set according to the desired proton's resonance frequency. For processing, the data was zero filled to 8192 points in F2 and 256 points in F1.

PROJECT[7] spectra: PROJECT spectra were recorded with 32768 data points (NS=4, DS=4) resulting in a FID resolution of about 0.75 Hz. 1024 loops for the T_2 filter were used with a cycle time (time of two echoes) of 1 ms. Zero filling was applied to 65536 data points in F2.

TSE-PSYCHE[8] spectra: TSE-PSYCHE spectra were acquired with 1024 data points and 128 time increments (300 ms long data chunks) in F1 (NS=32, DS=16).
A 30 ms PSYCHE element sweeping over 10 kHz with a flip angle of 20° was used. The selective 180° pulses were *RSnob*[5] pulses. The data was processed using the *pshift* macro (http://nmr.chemistry.manchester.ac.uk/sites/default/files/pshift).

Gradient-selected selective spin echo spectra: selgpse spectra (selgpse pulse sequence from Bruker's library) were recorded with 65536 data points (2.7 s acquisition time) (NS=2, DS=2). Selective refocusing was achieved using *RSnob*[5] 180° pulses with varying bandwidths. The offset was set according to the desired proton's resonance frequency. For processing, the data was zero filled to 131072 points.

SUPPORTING INFORMATION

S2.4 List of NMR Samples

A list of all samples used for the NMR experiments is given in Tables S1 and S2. The tables contain the name of the samples and the lab book identifiers (#) as well as the configuration and mass fraction (ω) of the chiral BTA of the system.

Table S1. NMR samples prepared with pure asymmetrically substituted BTA **2**.

Sample	#	$m_{BTA\ 2}$ / mg	$Configuration_{BTA}$	ω / %-w/w	Analyte	$m_{Analyte}$ / mg	m_{CDCl3} / mg
aS-(−)-β	ML98	140.92	S	22.99	(−)-β-pinene (−)-**1**	24.55	447.42
aS-(+)-β	ML99	140.60	S	23.20	(+)-β-pinene (+)-**1**	24.50	441.06
aR-(−)-β	ML100	140.99	R	24.49	(−)-β-pinene (−)-**1**	25.33	409.21
aR-(+)-β	ML101	141.27	R	24.46	(+)-β-pinene (+)-**1**	25.33	410.96

Table S2. NMR samples prepared with chiral BTA **3** (sergeant) and achiral BTA **4** (soldier).

Sample	#	$m_{BTA\ 4}$ / mg	$Configuration_{Sergeant}$	$m_{BTA\ 3}$ / mg	$\omega_{Sergeant}$ / %-w/w	Analyte	$m_{Analyte}$ / mg	m_{CDCl3} / mg
R1%-(+)-β	ML77	166.35	R	1.68	0.99	(+)-β-pinene (+)-**1**	25.42	420.60
R1%-(−)-β	ML79	170.29	R	1.72	0.99	(−)-β-pinene (−)-**1**	25.00	430.47
R3%-(+)-β	ML76	165.11	R	5.00	2.94	(+)-β-pinene (+)-**1**	25.42	426.63
R3%-(−)-β	ML75	164.98	R	5.01	2.95	(−)-β-pinene (−)-**1**	24.86	425.94
R5%-(+)-β	ML78	161.82	R	8.51	4.99	(+)-β-pinene (+)-**1**	25.33	425.68
R5%-(−)-β	ML80	161.35	R	8.49	4.99	(−)-β-pinene (−)-**1**	24.95	425.69
S1%-(+)-β	ML97	168.31	S	1.70	0.99	(+)-β-pinene (+)-**1**	25.10	425.88
S1%-(−)-β	ML91	168.32	S	1.70	0.99	(−)-β-pinene (−)-**1**	25.23	425.31
S3%-(+)-β	ML95	165.93	S	5.13	2.99	(+)-β-pinene (+)-**1**	25.22	428.43
S3%-(−)-β	ML92	164.39	S	5.08	2.99	(−)-β-pinene (−)-**1**	25.57	423.29
S5%-(+)-β	ML96	162.06	S	8.53	5.00	(+)-β-pinene (+)-**1**	25.31	426.18
S5%-(−)-β	ML93	161.12	S	8.48	5.00	(−)-β-pinene (−)-**1**	25.17	424.48

SUPPORTING INFORMATION

S2.5 Use of PROJECT and TSE-PSYCHE spectra to facilitate TSE-PSYCHEDELIC setup

The TSE-PSYCHEDELIC pulse sequence for the extraction of ^{1}H-^{1}H coupling magnitudes relies on selective refocusing of individual proton resonances. If the signals of the analyte are well resolved, even in the anisotropic phase, this can easily be done by selecting the resonance of the proton in question. But in the case of broadened and overlapping spectral lines, often encountered in the anisotropic state, the setup of the pulse for the selective refocusing is non-trivial as the observed chemical shift may be perturbed by a few Hz due to the contributions of the alignment medium to the baseline and phase corrections of the spectrum. In this study we combined the usage of PROJECT[7]-, TSE-PSYCHE[8]- and gradient-selected selective spin echo spectra (selgpse) to enable optimal refocusing of the proton resonances in the TSE-PSYCHEDELIC[4] experiment (example spectra shown for sample S5%-(+)-β in figure S1). For this approach standard ^{1}H spectra as a reference were recorded. As can be seen, the broad signals of the alignment medium disturb the already broadened lines of the analyte. Utilizing the PROJECT pulse sequence as a T_2 filter (relaxation filter) we were able to filter the broad signals of the alignment medium and obtain a spectrum dominated only by the signals of the analyte. To obtain the exact chemical shifts of the β-pinene protons, TSE-PSYCHE spectra were recorded, which allowed the extraction of the chemicals shifts as a result of its homodecoupling capabilities. Having obtained the chemical shifts of all protons of interest, selgpse spectra were used to optimize the pulse widths to refocus only the resonances of a single proton. In this process selgpse spectra were repeatedly overlaid with the PROJECT spectra to check for selectivity of the refocused line in the selgpse spectrum compared to the resonance in the PROJECT spectrum. These optimized pulse widths were then used in the 2D TSE-PSYCHEDELIC spectra to obtain the ^{1}H-^{1}H couplings.

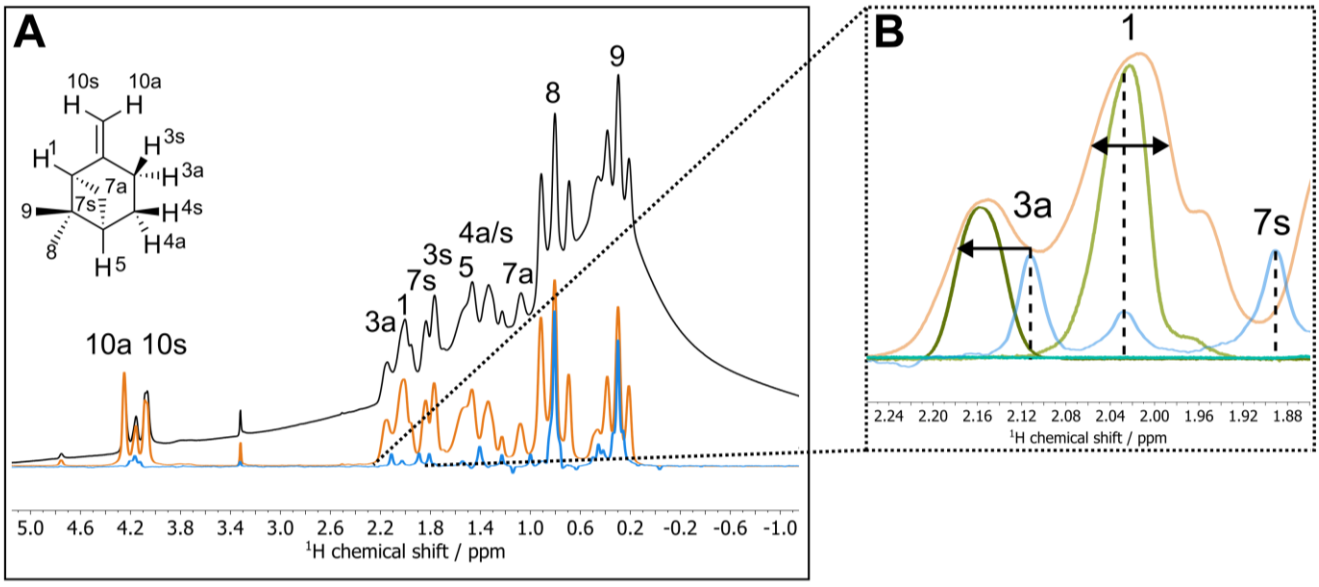

Figure S1. (**A**) Comparison of a standard ^{1}H spectrum (black), a ^{1}H-PROJECT spectrum (orange) and a TSE-PSYCHE spectrum (blue) of sample S5%-(+)-β Numbering of (+)-**1** as indicated by the structure. In **B** a zoom of the region between 2.24 ppm and 1.88 ppm is shown. Two selgpse spectra (dark green for proton 3a) and (green for proton 1) are overlayed with the ^{1}H-PROJECT spectrum (orange) and a TSE-PSYCHE spectrum (blue) to visualize the procedure of finding the optimal pulse width for the 2D TSE-PSYCHEDELIC as mentioned in S2.5. In the ideal case, only one resonance should be refocused by the selgpse spectrum corresponding to a peak of a multiplet in the ^{1}H-PROJECT spectrum (orange) that belongs to only one proton as implied by the pure shift resonance reference in the TSE-PSYCHE spectrum (blue).

S2.6 RDC analysis of β-pinene

The measurement and analysis of RDCs of β-pinene in the SaS BTA and asymmetrically substituted BTA systems is laid out below. Heteronuclear one bond ^{1}H-^{13}C RDCs as well as scalar coupling constants ($^{1}J_{CH}$) were extracted from Perfect-CLIP-HSQC-spectra.[3] The averaged RDCs of the methyl groups were converted to the corresponding ^{13}C-^{13}C-RDCs according to the method published by VERDIER et al..[9] Signs and magnitudes of the scalar coupling constants ($^{n}J_{HH}$) for β-pinene **1**, determined by ALCARAZ JANßEN et al.[10] and SINNAEVE et al.[4b], were used. The magnitudes of the homonuclear ^{1}H-^{1}H RDCs were obtained from 2D TSE-PSYCHEDELIC[4] spectra. Experimental errors were estimated as described by KUMMERLÖWE et al..[11] If the error determined for the ^{1}H-^{1}H RDC was smaller than the zero-filled spectral resolution of the 2D TSE-PSYCHEDELIC spectrum (0.09 Hz), an error of 0.1 Hz was used. Depending on the system, different methods were used to obtain a consistent set of signs for the proton total coupling ($^{n}T_{HH}$). For both BTA systems the sign of $T_{H1\text{-}H5}$ was determined by P.E.HSQMBC spectra, relative to the known positive coupling $^{1}J_{C5\text{-}H5}$. In addition to this sign, relative sign information for the other total coupling ($^{n}T_{HH}$) was obtained from CT-β-COSY spectra for the asymmetrically substituted BTA systems. The JUPYTER notebook published by SINNAEVE et al.[4b] was then used to check the consistency of the signs of all measured total coupling constants ($^{n}T_{HH}$) based on the relative sign information. The output is shown below.

SUPPORTING INFORMATION

Checking for contradictions in the known signs...
No contradictions found!
Checking for contradictions in the coupling relations...
No contradictions found!
Derive the signs...
Finished!
Checking for contradictions in the derived couplings...
No contradictions found!
Established coupling signs:

Coupling	Sign	History
H1-H5	positive	initially known sign
H5-H7a	positive	H5H1=1 | rel 2 -> H5H7a=+1
H1-H3a	negative	H5H1=1 | rel 5 -> H3aH1=-1
H1-H7s	positive	H5H1=1 | rel 8 -> H1H7s=+1
H3a-H7a	negative	H5H1=1 | rel 2 -> H5H7a=+1 | rel 4 -> H7aH3a=-1
H3s-H5	positive	H5H1=1 | rel 2 -> H5H7a=+1 | rel 7 -> H5H3s=+1
H5-H7s	positive	H5H1=1 | rel 2 -> H5H7a=+1 | rel 14 -> H5H7s=+1
H1-H7a	negative	H5H1=1 | rel 5 -> H3aH1=-1 | rel 19 -> H7aH1=-1
H3s-H7s	negative	H5H1=1 | rel 8 -> H1H7s=+1 | rel 17 -> H3sH7s=-1
H3s-H7a	positive	H5H1=1 | rel 2 -> H5H7a=+1 | rel 4 -> H7aH3a=-1 | rel 13 -> H7aH3s=+1
H3a-H5	positive	H5H1=1 | rel 2 -> H5H7a=+1 | rel 7 -> H5H3s=+1 | rel 12 -> H5H3a=+1
H3a-H7s	negative	H5H1=1 | rel 2 -> H5H7a=+1 | rel 14 -> H5H7s=+1 | rel 16 -> H3aH7s=-1
H1-H3s	negative	H5H1=1 | rel 5 -> H3aH1=-1 | rel 19 -> H7aH1=-1 | rel 9 -> H1H3s=-1
H7a-H7s	negative	H5H1=1 | rel 5 -> H3aH1=-1 | rel 19 -> H7aH1=-1 | rel 10 -> H7aH7s=-1
H3a-H3s	positive	H5H1=1 | rel 2 -> H5H7a=+1 | rel 14 -> H5H7s=+1 | rel 16 -> H3aH7s=-1 | rel 11 -> H3aH3s=+1

All relations were used.
No contradictions between the final signlist and the relation table were found.

The RDCs obtained in this way for the samples containing the asymmetrically substituted BTA **2** are listed in table S3.
In the case of the SaS BTA samples CT-β-COSY spectra were measured as well, but not enough relative sign information could be obtained. Thus, other ways of obtaining a consistent dataset were employed. The RDC@hotFCHT[12] software package was utilized for these systems to determine the signs of total couplings ($^nT_{HH}$) other than $T_{H1\text{-}H5}$. Using permutation of coupling signs and jackknifing[13], signs of the total couplings ($^nT_{HH}$) consistent with the ^{1}H-^{13}C RDCs were established. The best-fit solution of the SVD (singular value decomposition) and the corresponding sign permutation of only the ^{1}H-^{1}H-RDCs or the full ^{1}H-^{13}C- and ^{1}H-^{1}H-RDCs was checked for consistency using a leave-one-out cross-validation (jackknifing) approach. To achieve that, single ^{1}H-^{1}H-RDCs were removed from the combined ^{1}H-^{1}H- and ^{1}H-^{13}C-RDC dataset and the resulting sign permutations of the total couplings ($^nT_{HH}$) were compared to the best-fit solution of the full dataset. This way a sign permutation of the total couplings ($^nT_{HH}$) in agreement with the ^{1}H-^{13}C-RDCs and the best fit solution for the SVD of the full RDC set was obtained for all SaS BTA samples. The obtained RDCs for the SaS BTA systems are listed in table S7-8 and the orientation properties obtained in tables S9-10. It is worth noting that, it is essential for such comparisons to employ a consistent dataset for all samples. Here, the ^{1}H-^{13}C-RDCs of C4-H4a/s were not employed. This decision was made due to signal overlap and strong coupling effects, which vary between samples and prevent clean RDC extraction for some of the samples.
For the evaluation of the RDC data based on a structural model of (−)-β-pinene (−)-**1** (see section S2.7 for details) the RDC@hotFCHT[12] software package was used for all datasets. In the following sections, the condition number of the coefficient matrix is used to indicate the numerical sensitivity of the matrix inversion procedure (SVD). The Saupe tensor **S** (Alignment tensor **A** = 2/3·**S**) is described by its axial (D_a) and rhombic components (D_r), the generalized degree of order (GDO) and its orientation in the molecular frame reported by Euler angles (α, β, and γ) following the z(γ)-y'(β)-z''(α) convention. The root mean square deviation (RMSD) and quality factor Q[14] are used as a description for the quality of the fit procedure. We use Monte Carlo bootstrapping to assess the scattering of the alignment tensor as proposed by LOSONCZI et al..[15] For this, experimental RDCs are varied randomly within their experimental errors and the scattering of the eigenvectors of the obtained alignment tensor is displayed as points on the surface of a unit sphere. The eigenvectors of the best-fit solution for the set of experimental RDCs are shown as arrows. A narrow scattering of points from the Monte Carlo bootstrapping, around the best-fit eigenvectors, signifies a well-defined alignment tensor orientation. The eigenvectors of the Saupe matrix of β-pinene **1** in the asymmetrically substituted BTA **2** samples using all RDCs are shown in figure S3. For the eigenvectors of the Saupe matrix of β-pinene **1** in the SaS-BTA samples using all RDCs with varying sergeant concentration see figures S4-S6.

SUPPORTING INFORMATION

S2.7 Cartesian coordinates used for RDC fitting

The geometry of (−)-β-pinene was optimized by density functional theory (DFT) at the B3LYP[16]/def2-TZVP[17] level, as implemented in the ORCA 4.1.1 software package.[18]

(−)-β-pinene

26

bpinene

C	-4.035044	0.362146	-0.836658
C	-2.033479	-1.054174	-0.320932
C	-0.488959	-0.890053	-0.318503
C	-0.077608	0.518081	0.128486
C	-1.046963	0.995631	1.243328
C	-1.992713	1.447387	0.090026
C	-0.698806	1.619874	-0.799094
C	-0.809124	1.363273	-2.297828
C	-0.054690	2.996543	-0.595580
C	-2.783948	0.266344	-0.394512
H	0.996961	0.577028	0.318198
H	-0.653615	1.833601	1.813884
H	-1.428615	0.248304	1.940070
H	-1.270329	0.408202	-2.543883
H	0.179900	1.391660	-2.764563
H	-1.413984	2.142261	-2.769861
H	0.071260	3.264851	0.453226
H	-0.667195	3.771079	-1.065498
H	0.931862	3.028772	-1.066241
H	-2.618683	2.329649	0.234480
H	-2.333175	-1.548448	0.607934
H	-2.354303	-1.719557	-1.123962
H	-4.576485	-0.501967	-1.205017
H	-4.563521	1.308169	-0.838598
H	-0.075331	-1.102575	-1.306795
H	-0.049374	-1.625042	0.360675

S2.8 Spectral quality in asymmetrically substituted BTA 2

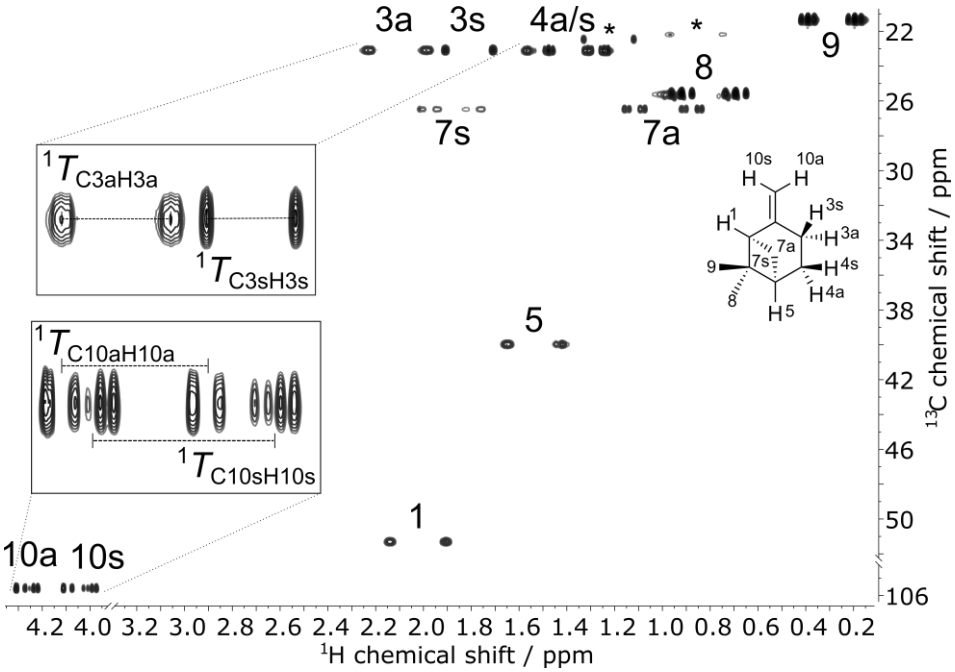

Figure S2. ^{1}H-^{13}C-Perfect-CLIP-HSQC spectrum of aR(+)-β (600 MHz ^{1}H frequency, 300 K). Excerpts in rectangles visualize exemplary total couplings ($^{1}T_{CH}$) of separated signals that can be extracted. ^{13}C-axis is cut to improve visibility of signals.

SUPPORTING INFORMATION

S3. RDC data

In this section RDCs for all LLC phases and associated data is presented. The condition number given is the condition number of the coefficient matrix. Euler angles within the tables carry the unit [°] and follow the counterclockwise active z(γ)-y'(β)-z''(α) convention.

S3.1 Asymmetrically substituted BTA 2

Table S3. Experimental RDCs of (+) or (−)-β-pinene ((+)-**1** or (−)-**1**) in the asymmetrically substituted BTA LLC phase of (*R*)-**2** or (*S*)-**2** in $CDCl_3$.See chapter S2.6 for details on sign determination of $^nT_{HH}$. Internal (LOGS) sample IDs are given in grey under the name of the sample.

RDC / Hz	aS-(+)-β		aR-(−)-β		aS-(−)-β		aR-(+)-β	
LOGS ID	394		517		393		518	
C1-H1	-4.29	±0.22	-4.32	±0.17	-1.02	±0.10	-0.92	±0.24
C3-H3a	7.63	±1.05	7.51	±1.69	10.16	±0.29	9.97	±0.17
C3-H3s	3.15	±0.58	3.72	±1.98	-4.36	±0.01	-4.77	±0.10
C5-H5	-1.56	±0.46	-1.81	±0.35	-4.45	±0.54	-4.72	±0.25
C7-H7a	-6.89	±0.85	-6.33	±0.32	2.80	±0.87	2.85	±0.16
C7-H7s	-12.15	±1.06	-12.81	±0.22	-12.44	±0.50	-12.92	±0.44
C8-C6	-2.26	±0.54	-2.16	±0.20	-1.58	±0.18	-1.52	±0.13
C9-C6	1.16	±0.94	1.45	±0.11	0.64	±0.10	0.85	±0.10
C10-H10a	-19.90	±0.49	-19.72	±0.36	-17.58	±0.54	-17.69	±0.38
C10-H10s	-12.64	±0.38	-12.48	±0.19	-4.47	±0.35	-4.50	±0.18
H1-H5	0.51	±0.10	0.48	±0.10	0.19	±0.10	0.21	±0.10
H5-H7a	4.38	±0.10	4.15	±0.10	2.06	±0.10	1.96	±0.10
H5-H7s	6.77	±0.10	6.81	±0.10	2.95	±0.10	2.94	±0.10
H3a-H7a	-4.77	±0.10	-4.73	±0.10	-5.63	±0.10	-5.60	±0.10
H3a-H7s	-1.45	±0.10	-1.64	±0.10	-1.20	±0.10	-1.25	±0.10
H3a-H3s	18.86	±0.10	18.75	±0.10	12.17	±0.10	12.03	±0.10
H1-H3a	-2.52	±0.10	-2.50	±0.10	-1.07	±0.10	-1.05	±0.10
H1-H3s	-0.82	±0.10	-0.98	±0.10	-0.43	±0.10	-0.47	±0.10
H1-H7a	-2.57	±0.10	-2.46	±0.10	-0.56	±0.10	-0.67	±0.10
H1-H7s	-0.16	±0.10	-0.16	±0.10	0.17	±0.10	0.17	±0.10

SUPPORTING INFORMATION

Table S4. Orientation properties obtained using C-H and H-H RDCs of (+) and (−)-β-pinene ((+)-**1** and (−)-**1**) in the asymmetrically substituted BTA LLC phase consisting of (*R*)-**2** and (*S*)-**2** in $CDCl_3$.

Sample	aS-(+)-β	aR-(−)-β	aS-(−)-β	aR-(+)-β
Quality factor Q	0.11	0.13	0.09	0.09
RMSD / Hz	0.89	1.01	0.57	0.57
Condition number	4.36	4.36	4.36	4.36
GDO [10^{-3}]	1.42	1.40	0.85	0.86
D_a [10^{-3}]	-0.65	-0.64	-0.37	-0.38
D_r [10^{-4}]	-3.35	-3.41	-2.38	-2.41
Euler angle α	159.16	159.11	176.33	176.33
Euler angle β	32.01	31.48	24.19	24.71
Euler angle γ	12.23	11.69	152.65	152.26

Table S5. Orientation properties obtained using datasets of only C-H RDCs of (+) or (−)-β-pinene ((+)-**1** or (−)-**1**) in the asymmetrically substituted BTA LLC phase of (*R*)-**2** or (*S*)-**2** in $CDCl_3$.

Sample	aS-(+)-β	aR-(−)-β	aS-(−)-β	aR-(+)-β
Quality factor Q	0.08	0.10	0.08	0.08
RMSD / Hz	0.72	0.96	0.61	0.62
Condition number	11.20	11.20	11.20	11.20
GDO [10^{-3}]	1.47	1.44	0.88	0.89
D_a [10^{-3}]	-0.66	-0.64	-0.39	-0.40
D_r [10^{-4}]	-3.74	-3.81	-2.33	-2.28
Euler angle α	156.72	156.12	174.22	172.89
Euler angle β	28.55	26.48	24.74	26.78
Euler angle γ	12.47	11.53	154.54	155.32

Table S6. Orientation properties obtained using datasets of only H-H RDCs of (+) or (−)-β-pinene ((+)-**1** or (−)-**1**) in the asymmetrically substituted BTA LLC phase of (*R*)-**2** or (*S*)-**2** in $CDCl_3$.

Sample	aS-(+)-β	aR-(−)-β	aS-(−)-β	aR-(+)-β
Quality factor Q	0.03	0.02	0.07	0.08
RMSD / Hz	0.18	0.11	0.31	0.33
Condition number	4.96	4.96	4.96	4.96
GDO [10^{-3}]	1.46	1.44	0.91	0.90
D_a [10^{-3}]	-0.63	-0.63	0.40	0.39
D_r [10^{-4}]	-4.13	-4.08	2.48	2.44
Euler angle α	163.77	162.80	67.82	67.98
Euler angle β	36.42	36.25	78.22	78.47
Euler angle γ	7.96	7.64	65.77	65.32

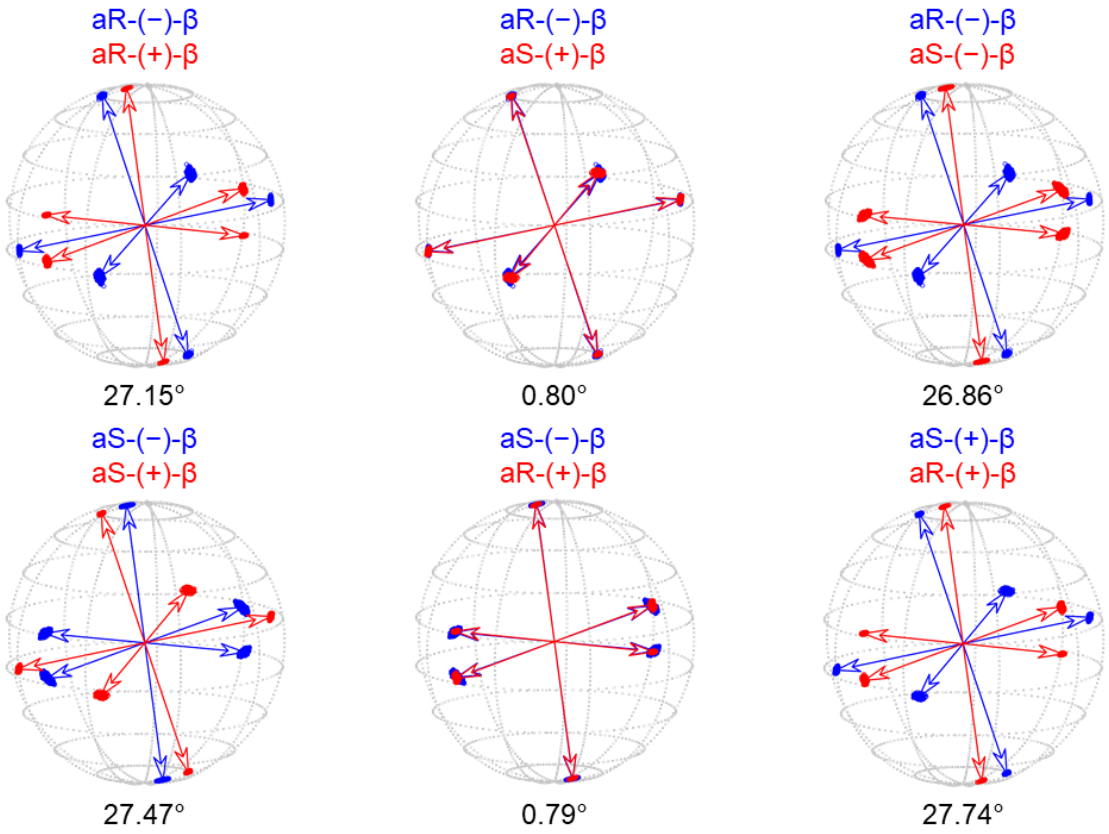

Figure S3. Eigenvectors of the Saupe matrix of β-pinene **1** in the ASYS-BTA system using all RDCs. The two visualizations in the center are enantiomorphous pairings: the configuration of the BTA and the analyte are both inverted, while in the outer pairings only one of the components is inverted, resulting in diastereomorphous pairings. For the enantiomorphous cases, the alignment is expected to be reproduced well, while the diastereomorphous cases show the capabilities of the chiral alignment medium to differentiate the enantiomers of β-pinene **1**. The β angles between the corresponding tensors are shown below the spheres. While the arrows represent the eigenvectors of the best-fit SVD-solution, scattered points show the spread of the eigenvectors during a Monte Carlo-boot-strapping within the range of the experimental RDC uncertainties.

S3.2 Sergeant and Soldier BTA 3/4

Table S7. Experimental RDCs of (+) or (−)-β-pinene ((+)-**1** or (−)-**1**) in the SaS BTA LLC phase of soldier **4** with 1% or 3% added sergeant (*R*)-**3** or (*S*)-**3** in $CDCl_3$ (Part 1). See chapter S2.6 for details on sign determination of $^nT_{HH}$. Internal (LOGS) sample IDs are given in grey under the name of the sample.

RDC / Hz	S1%-(+)-β		R1%-(−)-β		S1%-(−)-β		R1%-(+)-β		S3%-(+)-β		R3%-(−)-β	
LOGS ID	257		477		254		480		258		478	
C1-H1	-1.62	±0.20	-1.61	±0.84	0.56	±0.20	1.10	±0.38	-2.43	±0.22	-2.12	±0.05
C5-H5	-4.62	±0.82	-5.00	±0.30	-8.22	±0.31	-8.44	±0.57	-4.23	±2.37	-3.53	±0.49
C7-H7a	-13.01	±0.46	-12.73	±1.15	-4.98	±2.22	-4.36	±0.78	-14.14	±1.75	-13.89	±1.06
C7-H7s	-24.71	±1.37	-24.19	±1.05	-26.87	±1.23	-26.31	±1.16	-24.22	±0.89	-23.44	±0.87
C8-C6	-4.13	±0.23	-3.82	±0.43	-3.38	±0.47	-3.37	±0.26	-3.79	±1.18	-3.77	±0.32
C9-C6	2.97	±0.38	2.98	±0.26	2.19	±0.92	2.41	±0.14	3.51	±1.15	3.01	±0.56
C3-H3a	11.29	±0.83	11.43	±1.28	15.86	±1.84	15.04	±0.74	10.51	±0.76	9.93	±0.71
C3-H3s	2.41	±0.28	1.93	±0.25	-3.85	±1.46	-3.88	±0.86	3.52	±1.91	4.11	±1.07
H1-H5	0.67	±0.10	0.67	±0.10	0.61	±0.10	0.55	±0.10	0.79	±0.10	0.73	±0.10
H3a-H7a	-8.53	±0.10	-8.52	±0.10	-9.65	±0.10	-9.56	±0.10	-8.15	±0.10	-7.92	±0.10
H1-H3a	-3.47	±0.10	-3.31	±0.10	-2.69	±0.10	-2.64	±0.10	-3.63	±0.10	-3.53	±0.10
H1-H3s	-1.55	±0.10	-1.61	±0.10	-1.30	±0.10	-1.34	±0.10	-1.59	±0.10	-1.54	±0.10
H5-H7a	4.09	±0.10	3.98	±0.10	3.87	±0.10	3.76	±0.10	4.36	±0.10	4.06	±0.10
H5-H7s	9.59	±0.10	9.91	±0.10	9.00	±0.10	8.96	±0.10	10.16	±0.10	9.94	±0.10
H5-H3a	-2.35	±0.10	-2.42	±0.10	-2.25	±0.10	-2.27	±0.10	-2.29	±0.10	-2.36	±0.10
H5-H3s	-1.82	±0.10	-1.80	±0.10	-1.93	±0.10	-1.99	±0.10	-1.56	±0.10	-1.69	±0.10
H1-H7s	1.83	±0.10	1.78	±0.10	0.55	±0.10	0.42	±0.10	1.97	±0.10	1.88	±0.10

SUPPORTING INFORMATION

Table S8. Experimental RDCs of (+) or (−)-β-pinene ((+)-**1** or (−)-**1**) in the SaS BTA system LLC phase of soldier **4** with 3% or 5% added sergeant (*R*)-**3** or (*S*)-**3** in $CDCl_3$ (Part 2). See chapter S2.6 for details on sign determination of $^{n}T_{HH}$. Internal (LOGS) sample IDs are given in grey under the name of the sample.

RDC / Hz	S3%-(−)-β		R3%-(+)-β		S5%-(+)-β		R5%-(−)-β		S5%-(−)-β		R5%-(+)-β	
LOGS ID	255		479		259		476		256		481	
C1-H1	1.63	±0.19	1.43	±0.64	-2.44	±1.56	-2.30	±0.19	1.26	±1.50	1.77	±0.12
C5-H5	-8.99	±0.73	-8.51	±0.43	-2.14	±0.32	-3.53	±0.68	-8.71	±0.62	-8.78	±0.74
C7-H7a	-2.01	±0.51	-2.48	±0.20	-13.94	±0.42	-14.02	±1.45	-1.46	±0.31	-2.17	±1.35
C7-H7s	-25.64	±1.24	-25.50	±0.97	-23.72	±0.75	-22.95	±1.07	-26.55	±1.07	-26.21	±1.38
C8-C6	-3.28	±0.44	-3.12	±0.84	-3.80	±0.60	-3.86	±0.26	-3.09	±0.14	-3.10	±0.24
C9-C6	2.22	±0.22	2.15	±0.38	3.04	±0.22	2.83	±0.38	2.15	±0.12	2.12	±0.15
C3-H3a	15.27	±1.04	15.22	±0.43	9.53	±0.32	9.80	±0.84	14.92	±1.37	15.42	±1.16
C3-H3s	-4.10	±1.68	-4.99	±0.42	3.56	±2.57	3.77	±0.25	-6.68	±0.47	-5.49	±0.77
H1-H5	0.62	±0.10	0.55	±0.10	0.82	±0.10	0.83	±0.10	0.55	±0.10	0.57	±0.10
H3a-H7a	-9.94	±0.10	-9.39	±0.10	-7.97	±0.10	-7.74	±0.10	-9.71	±0.10	-9.69	±0.10
H1-H3a	-2.66	±0.10	-2.23	±0.10	-3.56	±0.10	-3.53	±0.10	-2.23	±0.10	-2.25	±0.10
H1-H3s	-1.23	±0.10	-1.21	±0.10	-1.54	±0.10	-1.60	±0.10	-1.28	±0.10	-1.23	±0.10
H5-H7a	3.70	±0.10	3.62	±0.10	4.45	±0.10	4.41	±0.10	3.66	±0.10	3.67	±0.10
H5-H7s	8.54	±0.10	8.26	±0.10	10.19	±0.10	9.97	±0.10	8.13	±0.10	8.09	±0.10
H5-H3a	-2.25	±0.10	-2.17	±0.10	-2.31	±0.10	-2.29	±0.10	-2.02	±0.10	-2.07	±0.10
H5-H3s	-1.95	±0.10	-1.80	±0.10	-1.65	±0.10	-1.58	±0.10	-1.86	±0.10	-1.85	±0.10
H1-H7s	0.24	±0.10	0.27	±0.10	1.78	±0.10	1.80	±0.10	0.24	±0.10	0.19	±0.10

SUPPORTING INFORMATION

Table S9. Orientation properties obtained using combined datasets of C-H and H-H RDCs of (+) or (–)-β-pinene ((+)-**1** or (−)-**1**) in the SaS BTA LLC phase of soldier **4** with 1%, 3% or 5% added sergeant (*R*)-**3** or (*S*)-**3** in $CDCl_3$.

Sample	S1%-(+)-β	R1%-(−)-β	S1%-(−)-β	R1%-(+)-β	S3%-(+)-β	R3%-(−)-β	S3%-(−)-β	R3%-(+)-β	S5%-(+)-β	R5%-(−)-β	S5%-(−)-β	R5%-(+)-β
Quality factor Q	0.12	0.11	0.09	0.11	0.13	0.14	0.13	0.10	0.14	0.13	0.11	0.11
RMSD / Hz	1.00	0.91	0.86	0.94	1.08	1.09	1.10	0.88	1.13	1.01	0.98	0.91
Condition number	4.90	4.90	4.90	4.90	4.90	4.90	4.90	4.90	4.90	4.90	4.90	4.90
GDO [10^{-3}]	2.31	2.28	2.05	1.98	2.38	2.30	1.86	1.84	2.30	2.29	1.80	1.84
D_a [10^{-3}]	1.04	1.03	0.91	0.88	1.07	1.04	0.82	0.82	1.04	1.03	0.81	0.82
D_r [10^{-4}]	5.69	5.75	5.45	5.29	6.07	5.75	5.07	4.88	5.74	5.82	4.65	4.80
Euler angle α	66.99	66.91	62.09	61.36	68.49	68.41	59.81	60.16	69.78	68.86	59.71	59.59
Euler angle β	91.79	91.68	86.20	85.86	92.79	92.98	84.45	84.37	93.24	93.14	83.22	83.91
Euler angle γ	67.40	66.83	66.00	65.48	66.33	66.83	65.79	65.74	64.96	66.03	65.54	65.93

Table S10. Orientation properties obtained using datasets of only C-H RDCs of (+) or (−)-β-pinene ((+)-**1** or (−)-**1**) in the SaS BTA LLC phase of soldier **4** with 1%, 3% or 5% added sergeant (*R*)-**3** or (*S*)-**3** in $CDCl_3$.

Sample	S1%-(+)-β	R1%-(−)-β	S1%-(−)-β	R1%-(+)-β	S3%-(+)-β	R3%-(−)-β	S3%-(−)-β	R3%-(+)-β	S5%-(+)-β	R5%-(−)-β	S5%-(−)-β	R5%-(+)-β
Quality factor Q	0.06	0.05	0.06	0.06	0.05	0.07	0.08	0.06	0.07	0.06	0.04	0.06
RMSD / Hz	0.63	0.49	0.66	0.63	0.56	0.78	0.86	0.63	0.77	0.64	0.42	0.65
Condition number	46.85	46.85	46.85	46.85	46.85	46.85	46.85	46.85	46.85	46.85	46.85	46.85
GDO [10^{-3}]	4.19	3.90	3.36	3.72	4.56	4.40	3.80	3.36	4.51	4.17	4.21	3.54
D_a [10^{-3}]	-2.04	-1.89	-1.63	-1.82	-2.22	-2.14	-1.86	-1.64	-2.20	-2.03	-2.06	-1.73
D_r [10^{-4}]	-5.45	-5.24	-4.46	-4.55	-5.89	-5.70	-4.60	-4.02	-5.62	-5.41	-5.01	-4.16
Euler angle α	145.16	145.30	140.38	139.70	145.43	145.70	138.39	138.58	145.76	146.08	137.83	138.23
Euler angle β	142.07	142.63	142.49	140.90	141.63	141.65	140.12	140.91	141.14	142.04	138.89	140.37
Euler angle γ	32.33	28.77	19.48	29.35	37.59	37.41	34.51	26.11	39.77	34.84	41.45	28.83

Table S11. Orientation properties obtained using datasets of only H-H RDCs of (+) or (−)-β-pinene ((+)-**1** or (−)-**1**) in the SaS BTA LLC phase of soldier **4** with 1%, 3% or 5% added sergeant (*R*)-**3** or (*S*)-**3** in $CDCl_3$.

Sample	S1%-(+)-β	R1%-(−)-β	S1%-(−)-β	R1%-(+)-β	S3%-(+)-β	R3%-(−)-β	S3%-(−)-β	R3%-(+)-β	S5%-(+)-β	R5%-(−)-β	S5%-(−)-β	R5%-(+)-β
Quality factor Q	0.02	0.01	0.02	0.02	0.02	0.02	0.03	0.02	0.02	0.01	0.02	0.02
RMSD / Hz	0.09	0.06	0.11	0.09	0.09	0.08	0.16	0.09	0.07	0.07	0.09	0.09
Condition number	5.39	5.39	5.39	5.39	5.39	5.39	5.39	5.39	5.39	5.39	5.39	5.39
GDO [10^{-3}]	2.39	2.39	2.14	2.15	2.43	2.40	2.09	1.99	2.41	2.38	1.94	1.94
D_a [10^{-3}]	1.07	1.07	0.95	0.95	1.09	1.08	0.93	0.80	1.08	1.07	0.87	0.87
D_r [10^{-4}]	6.16	6.10	5.59	5.73	6.04	6.15	5.51	5.39	6.11	6.03	4.92	4.95
Euler angle α	67.52	66.49	61.46	60.78	69.41	68.33	59.78	62.39	69.64	70.01	59.53	59.39
Euler angle β	89.99	90.10	84.77	84.61	91.72	91.50	83.09	83.46	91.86	92.08	82.17	82.09
Euler angle γ	68.12	67.35	66.28	67.18	65.71	67.14	67.80	65.75	65.18	65.55	66.22	66.41

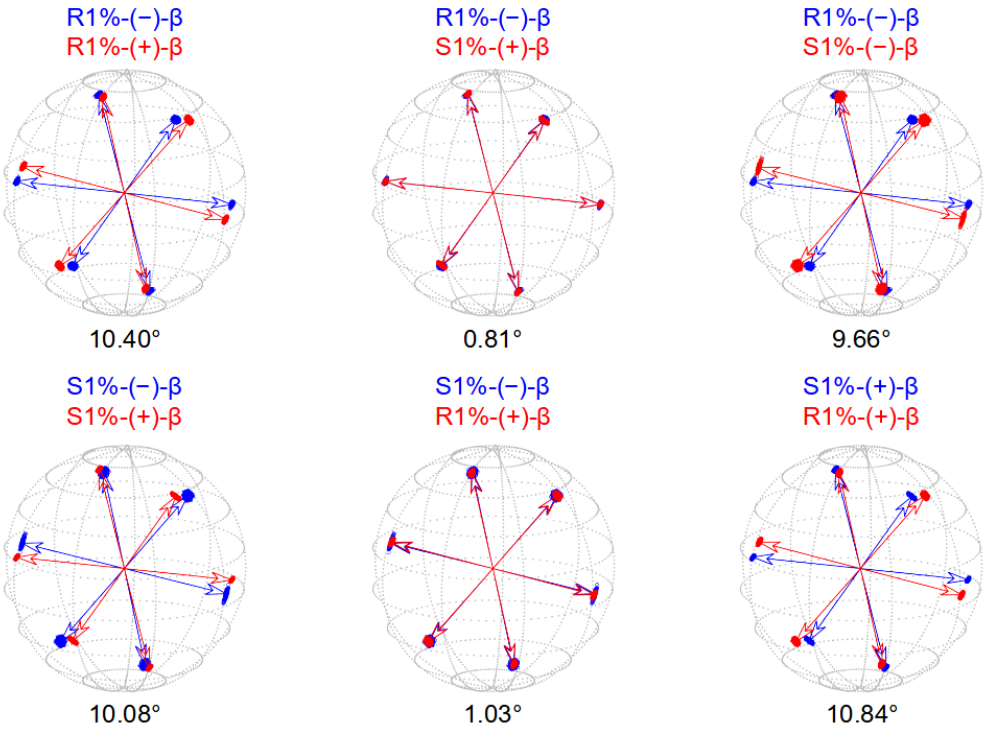

Figure S4. Eigenvectors of the Saupe matrix of β-pinene **1** in the SaS-BTA system using all combined datasets of C-H- and H-H-RDCs with 1% sergeant. The two visualizations in the center are enantiomorphous pairings: the configuration of the BTA and the analyte are both inverted, while in the outer pairings only one of the components is inverted, resulting in diastereomorphous pairings. For the enantiomorphous cases, the alignment is expected to be reproduced well, while the diastereomorphous cases show the capabilities of the chiral alignment medium to differentiate the enantiomers of β-pinene **1**. The β angles between the corresponding tensors are shown below the spheres. While the arrows represent the eigenvectors of the best-fit SVD-solution, scattered points show the spread of the eigenvectors during a Monte Carlo-boot-strapping within the range of the experimental RDC uncertainties.

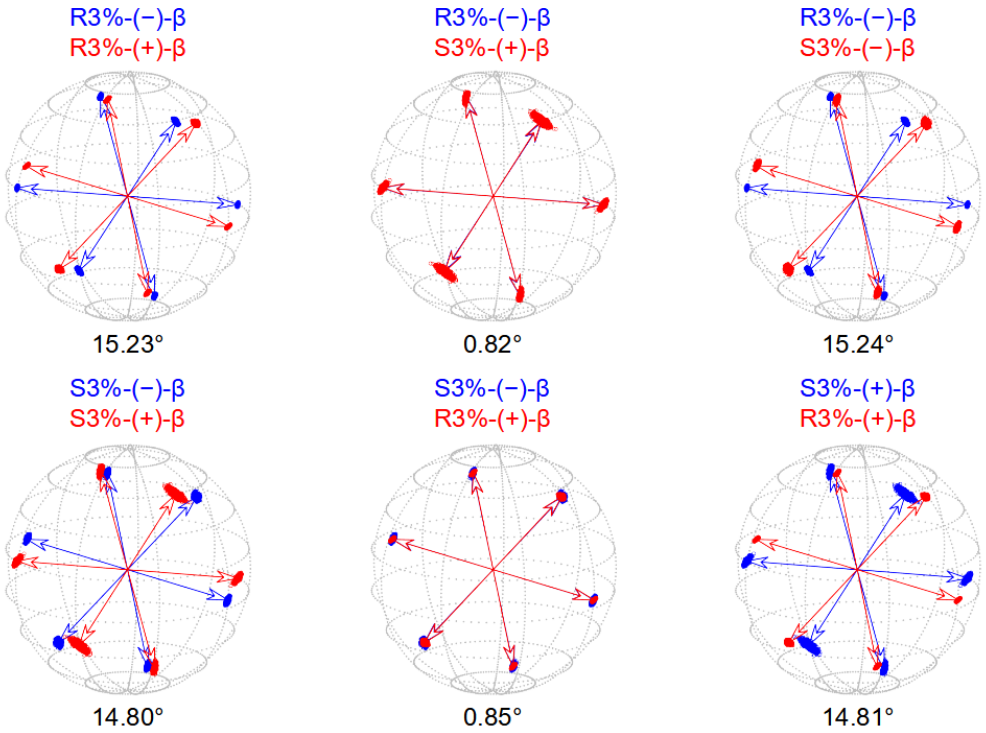

Figure S5. Eigenvectors of the Saupe matrix of β-pinene **1** in the SaS-BTA system using all combined datasets of C-H- and H-H-RDCs with 3% sergeant. The two visualizations in the center are enantiomorphous pairings: the configuration of the BTA and the analyte are both inverted, while in the outer pairings only one of the components is inverted, resulting in diastereomorphous pairings. For the enantiomorphous cases, the alignment is expected to be reproduced well, while the diastereomorphous cases show the capabilities of the chiral alignment medium to differentiate the enantiomers of β-pinene **1**. The β angles between the corresponding tensors are shown below the spheres. While the arrows represent the eigenvectors of the best-fit SVD-solution, scattered points show the spread of the eigenvectors during a Monte Carlo-boot-strapping within the range of the experimental RDC uncertainties.

SUPPORTING INFORMATION

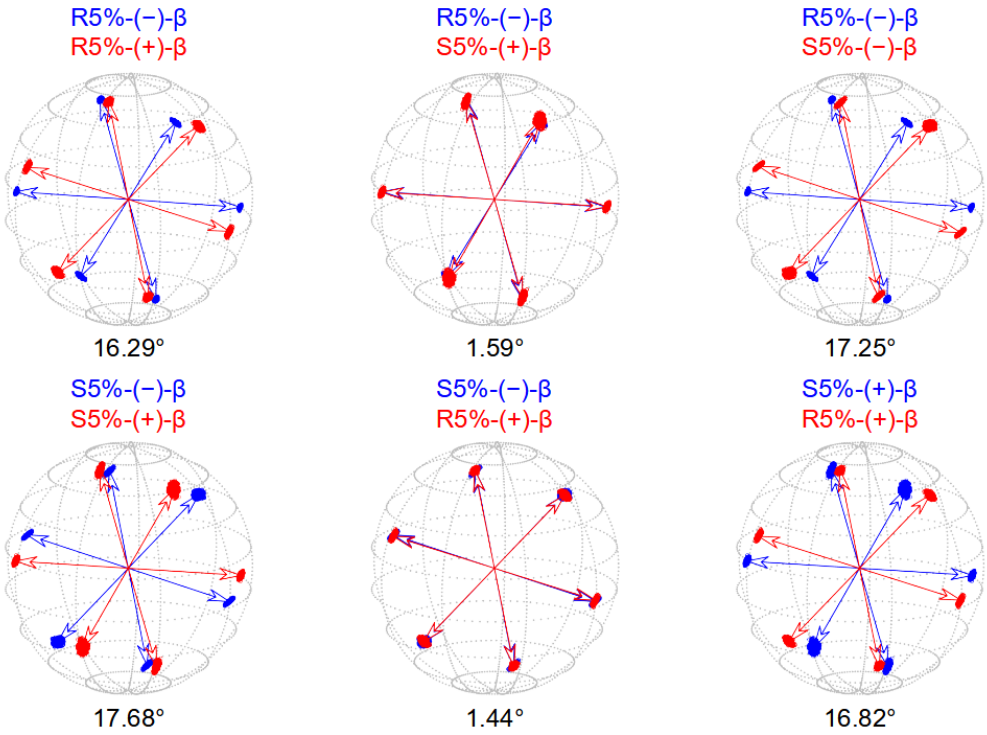

Figure S6. Eigenvectors of the Saupe matrix of β-pinene **1** in the SaS-BTA system using all combined datasets of C-H- and H-H-RDCs with 5% sergeant. The two visualizations in the center are enantiomorphous pairings: the configuration of the BTA and the analyte are both inverted, while in the outer pairings only one of the components is inverted, resulting in diastereomorphous pairings. For the enantiomorphous cases, the alignment is expected to be reproduced well, while the diastereomorphous cases show the capabilities of the chiral alignment medium to differentiate the enantiomers of β-pinene **1**. The β angles between the corresponding tensors are shown below the spheres. While the arrows represent the eigenvectors of the best-fit SVD-solution, scattered points show the spread of the eigenvectors during a Monte Carlo-boot-strapping within the range of the experimental RDC uncertainties.

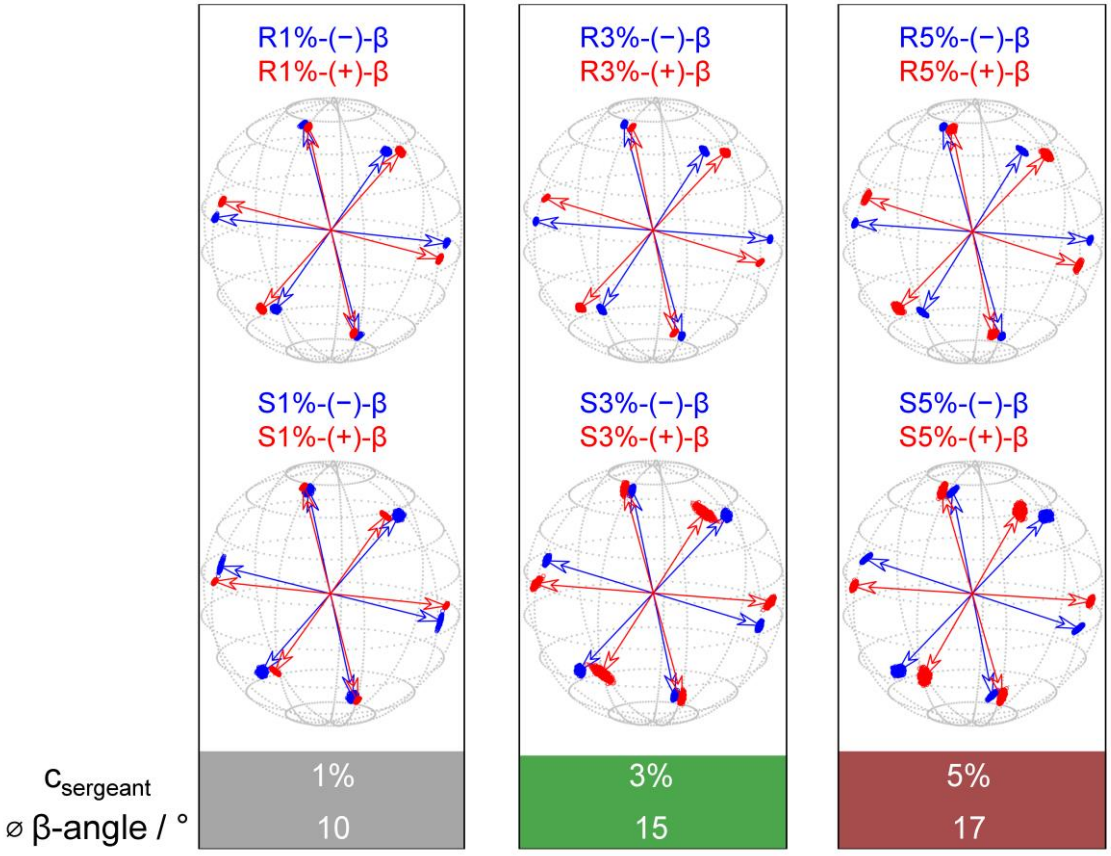

Figure S7. Comparison of eigenvectors of the Saupe matrix of β-pinene 1 in the SaS-BTA system using all RDCs with 1% (grey), 3% (green) and 5% (red) sergeant. The two visualizations shown per concentration of sergeant are diastereomorphous pairings in which the configuration of the BTA (upper sphere vs. lower sphere) or the analyte (within each sphere) is inverted. These diastereomorphous cases show the capabilities of the chiral alignment medium to differentiate the enantiomers of β-pinene 1. The averaged (⌀) β angles between the corresponding tensors are shown below the spheres and indicate the scalability.

SUPPORTING INFORMATION

S4. Synthesis and characterization of compounds

S4.1 *N*^{1},*N*^{3},*N*^{5}-tri((*S*)-Octan-2-yl)benzene-1,3,5-tricarboxamide (*S*)-3

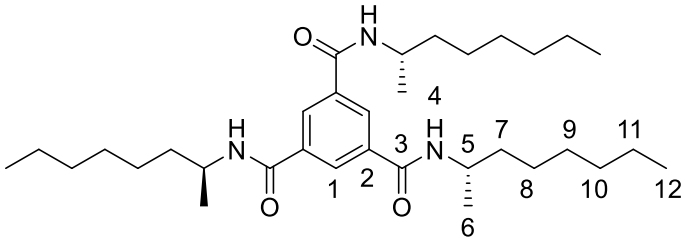

Synthesis of N^1,N^3,N^5-tri((*S*)-octan-2-yl)benzene-1,3,5-tricarboxamide (*S*)-**3:** N^1,N^3,N^5-tri((*S*)-octan-2-yl)benzene-1,3,5-tricarboxamide (*S*)-**3** was synthesized according to the procedure described for the *R* enantiomer (*R*)-**3**.[1] The product was obtained as a colorless solid (73.2 %).

^{1}H-NMR (600 MHz, 300 K, [D$_8$]THF): δ=8.34 (s, 3-H$_1$), 7.64 (d, 3-N-H$_4$, J = 8.15 Hz), 4.16 (m, 3-H$_5$), 1.60 (m, 3-H$_7$), 1.50 (m, 3-H$_7$), 1.42-1.27 (m, 25-H$_{8\text{-}11,}$ calc. 24, found 25), 1.20 (d, 9-H$_6$, J = 6.67 Hz), 0.89 (t, 9-H$_{12}$, J = 7.05 Hz) ppm ^{13}C-NMR (150 MHz, 300 K, [D$_8$]THF): δ=165.68 (C$_3$), 136.63 (C$_2$), 128.63 (C$_1$), 46.14 (C$_5$), 37.45 (C$_7$), 32.62 (C$_{10}$), 30.06 (C$_9$), 27.13 (C$_8$), 23.34 (C$_{11}$), 21.02 (C$_6$), 14.21 (C$_{12}$) ppm. HRMS (ESI): m/z calc. for $C_{33}H_{57}N_3O_3$+H$^+$: 544.4478 [M+H]$^+$; found: 544.4477; [α]D20=-57 (β=1.13·10^{-3} g/mL in DMSO);

^{1}H-NMR

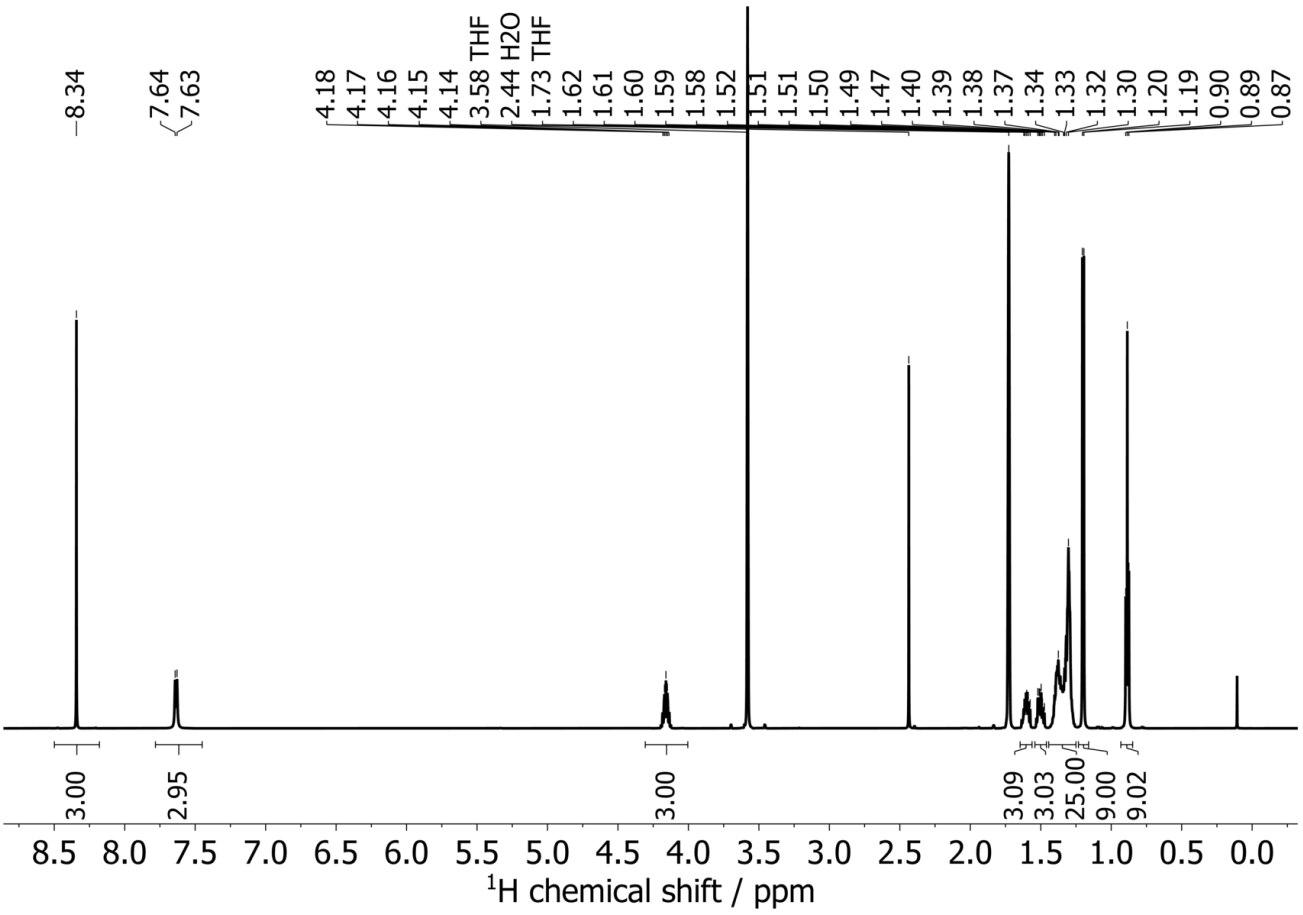

^{13}C-NMR

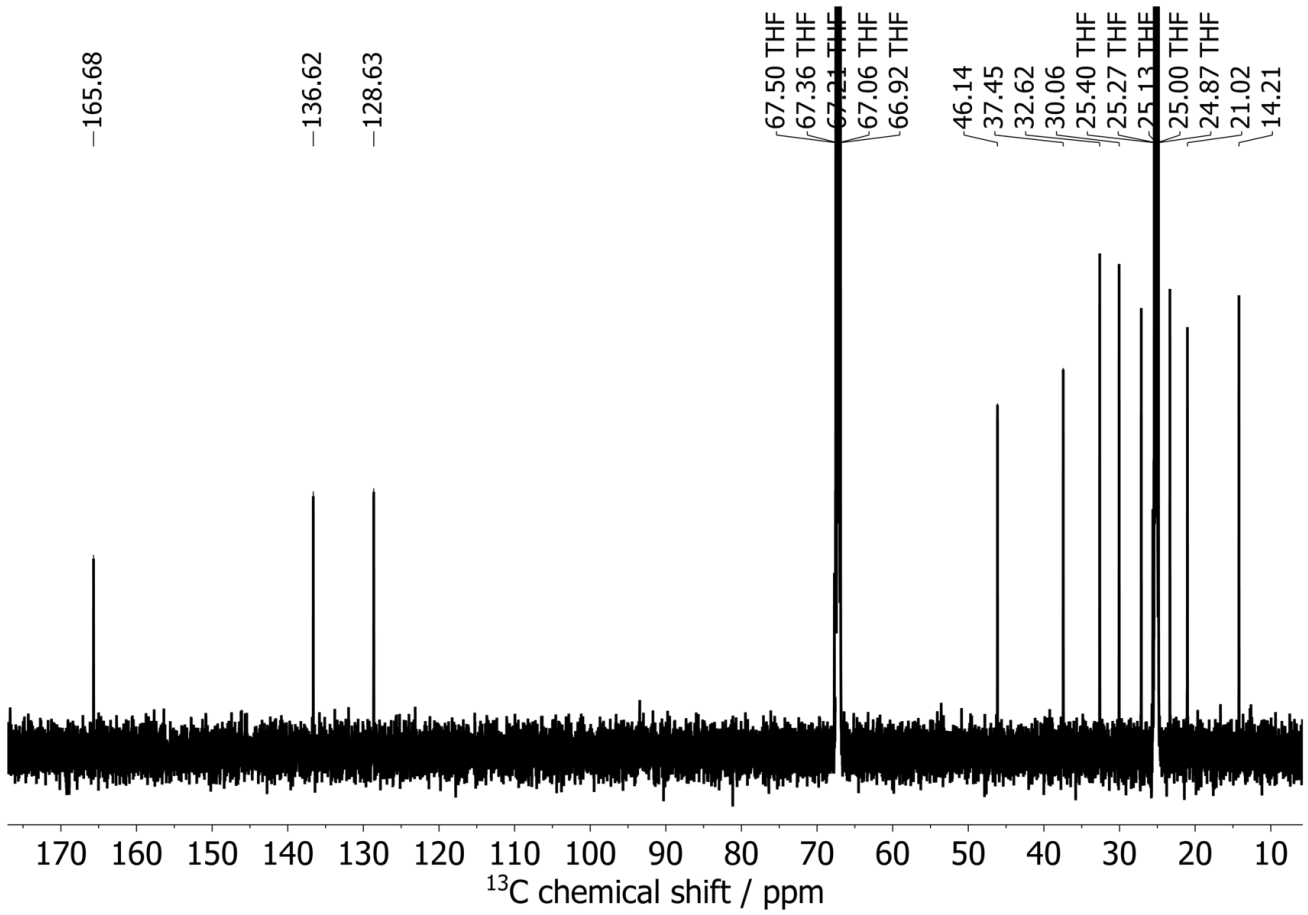

HRMS(ESI^{+})

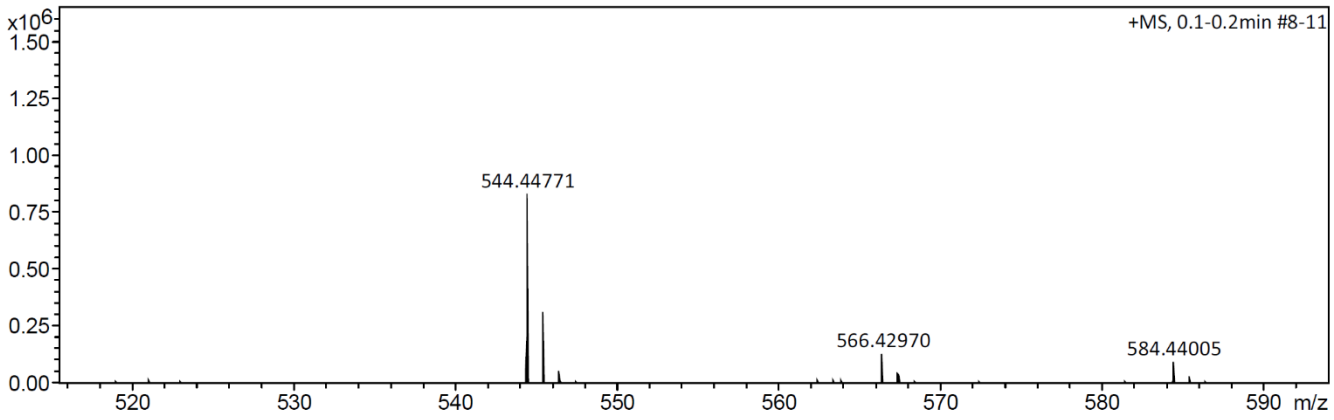

S4.2 Methyl 3,5-bis(dodecylcarbamoyl)benzoate 9

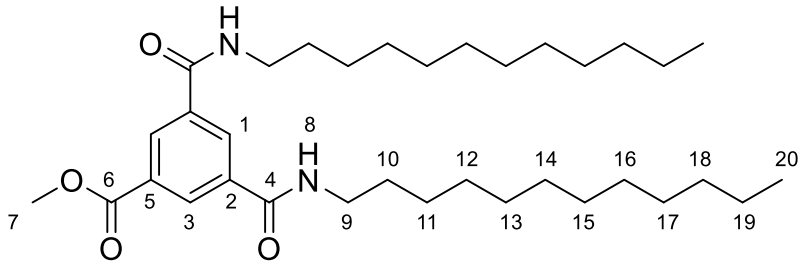

Synthesis of methyl 3,5-bis(dodecylcarbamoyl)benzoate 9:

9 was prepared by dissolving 3.459 g 5-(methoxycarbonyl)isophthalic acid **6** under argon atmosphere in 100 mL dry THF. The solution was cooled to 0 °C and 5.056 g 1,1'-carbonyldiimidazole **8** (31.2 mmol, 2.02 eq.) were added. The solution was stirred at room temperature for 28.5 h. Afterwards 5.906 g dodecylamine **7** (31.2 mmol 2.02 eq.) were dissolved in 55 mL dry THF and added to the above solution over 30 min at 0 °C. The solution was stirred at room temperature for 66 h. After removal of the solvent under vacuum, 13.085 g of the raw yellow product were obtained. The raw product was used in the next synthesis without purification.
R_f = 0.52 (petroleum ether/EtOAc/glacial acetic acid ratio 15:15:0.1);

^{1}H-NMR (700 MHz, 300 K, [D_8]THF): δ=8.54 (d, 2-H_3, ^4J = 1.71 Hz), 8.52 (t, 1-H_1, ^4J = 1.70 Hz), 7.97 (t, 2-N-H_8, J = 5.45 Hz), 3.90 (s, 3-H_7), 3.38 (m, 4-H_9), 1.60 (m, 4-H_{10}), 1.40 – 1.27 (m, 39-$H_{11–19}$, calc. 36, found 39), 0.89 (t, 6-H_{20}, J = 7.12 Hz) ppm; ^{13}C-NMR (175 MHz, 300 K, [D_8]THF): δ=166.27 (C_6), 165.45 (C_4), 136.87 (C_2), 131.18 (C_5); 130.93 (C_1), 130.62 (C_3), 52.21 (C_7), 40.50 (C_9), 30.54 (C_{10}), 27.83 (C_{11}), 32.68, 30.45 – 30.41, 30.27, 30.12, 23.37 ($C_{12–19}$), 14.24 (C_{20}) ppm.

^{1}H-NMR

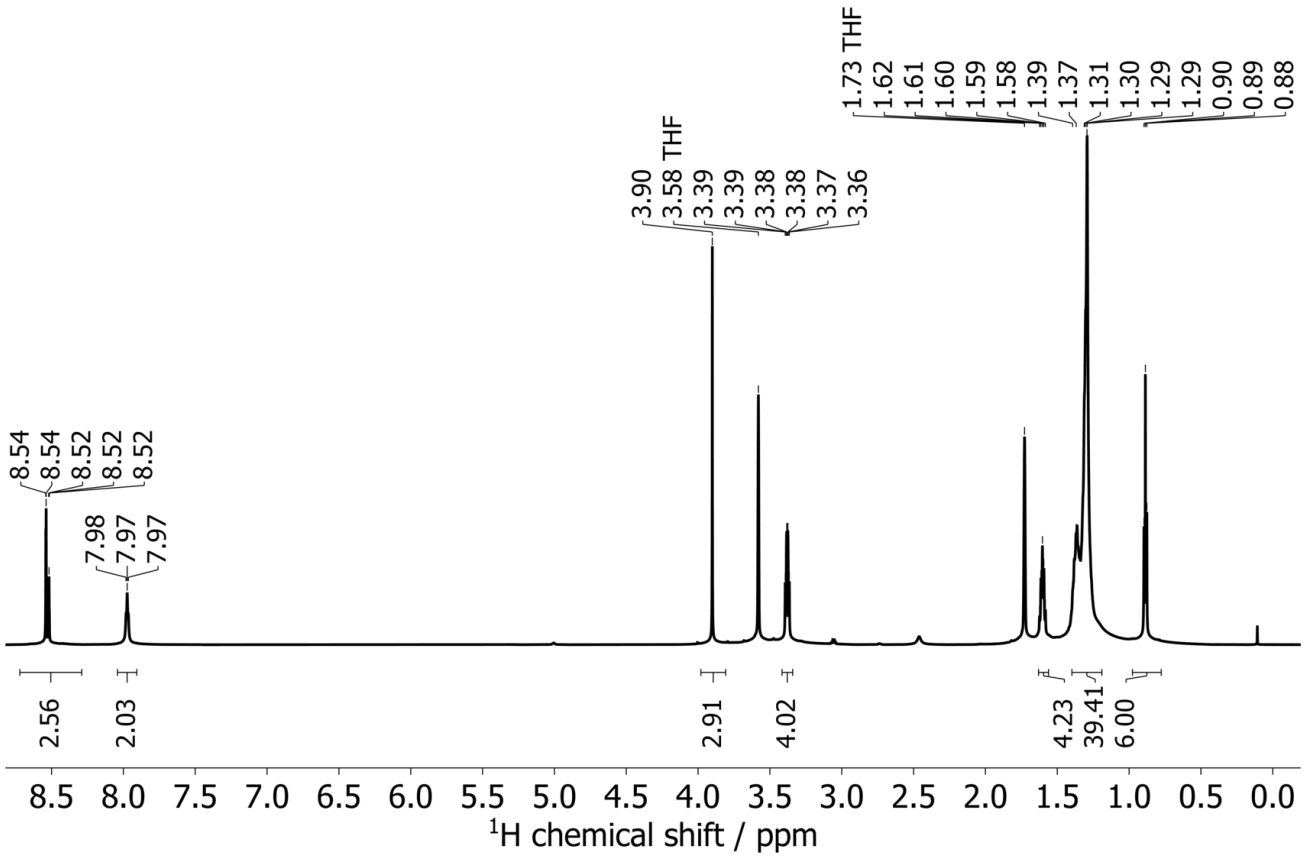

^{13}C-NMR

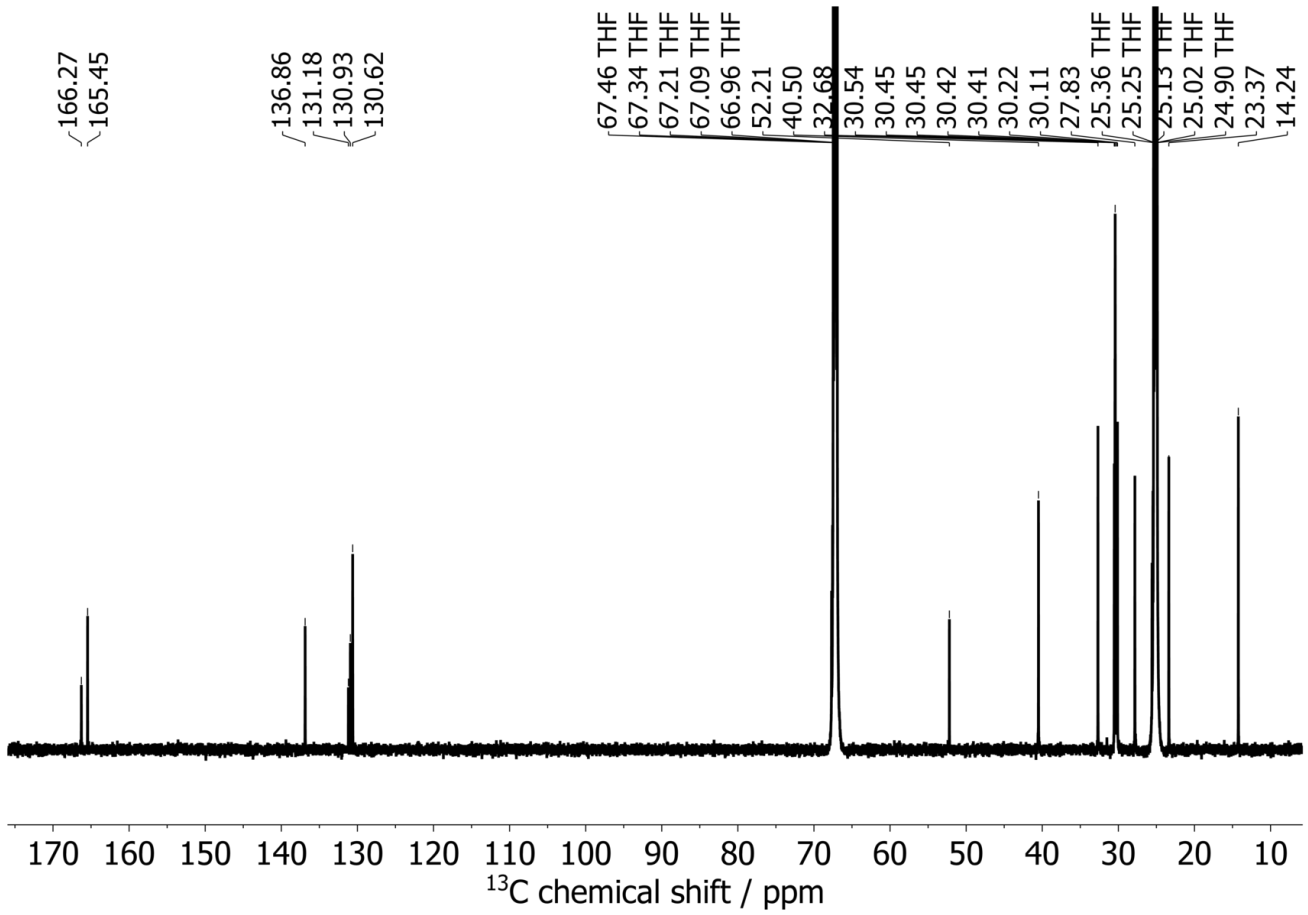
166.27
165.45
136.86
131.18
130.93
130.62
67.46 THF
67.34 THF
67.21 THF
67.09 THF
66.96 THF
52.21
40.50
32.68
30.54
30.45
30.45
30.42
30.41
30.22
30.11
27.83
25.36 THF
25.25 THF
25.13 THF
25.02 THF
24.90 THF
23.37
14.24
170 160 150 140 130 120 110 100 90 80 70 60 50 40 30 20 10
^{13}C chemical shift / ppm

S4.3 3,5-Bis(dodecylcarbamoyl)benzoic acid 10

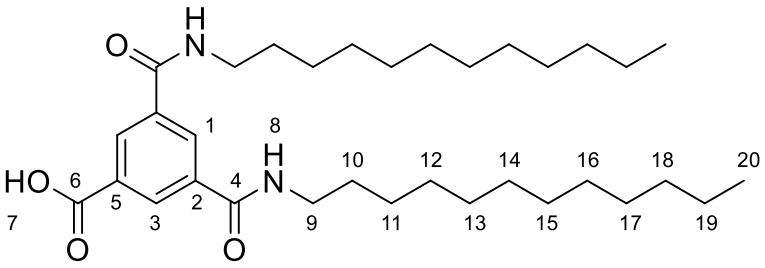

Synthesis of 3,5-bis(dodecylcarbamoyl)benzoic acid (10):

10 was prepared by suspending 12.44 g methyl 3,5-bis(dodecylcarbamoyl)-benzoate (**9**) and 0.934 g (22 mmol, 1.5 eq based on 5-(methoxycarbonyl)isophthalic acid **6**) $LiOH \cdot H_2O$ in 400 mL methanol as well as 11.5 mL water. The reaction mixture is stirred at 60 °C for 21 h. Afterwards the solution was poured into 800 mL 1M HCl. The precipitated product was filtered off and washed two times with 100 mL 1 M HCl. 7.756 g of the raw light-yellow product were obtained. The raw product is recrystallized from 35 mL methanol and washed two times with 10 mL cold methanol (-90 °C). After removal of the solvent the product (5.945 g, 70.7% over two steps) is obtained as a colorless crystalline powder.
R_f = 0.0 (petroleum ether/EtOAc 1:1);

^{1}H-NMR (600 MHz, 300 K, [D_8]THF): δ=11.68 (bs, 1-H_7); 8.55 (d, 2-H_3, ^4J = 1.71 Hz); 8.50 (t, 1-H_1, ^4J = 1.71 Hz); 7.96 (t, 2-N-H_8, J = 5.53 Hz); 3.38 (m, 4-H_9); 1.60 (m, 4-H_{10}); 1.41 – 1.26 (m, 39-$H_{11–19}$, calc. 36, found 39); 0.89 (t, 6-H_{20}, J = 7.09 Hz) ppm; ^{13}C-NMR (150 MHz, 300 K, [D_8]THF): δ=166.81 (C_6), 165.63 (C_4), 136.75 (C_2), 131.82 (C_5), 130.88 (C_3), 130.76 (C_1), 40.48(C_9), 30.55 (C_{10}), 27.84 (C_{11}), 32.68, 30.44 – 30.40, 30.22, 30.12, 23.36 ($C_{12–19}$), 14.23 (C_{20}) ppm; HRMS (ESI): m/z calc. for $C_{33}H_{56}N_2O_4$+H^+: 545.4313 $[M+H]^+$; found: 545.4314; [α]D20=0 (β=1.17·10^{-3} g/mL in DMSO);

^{1}H-NMR

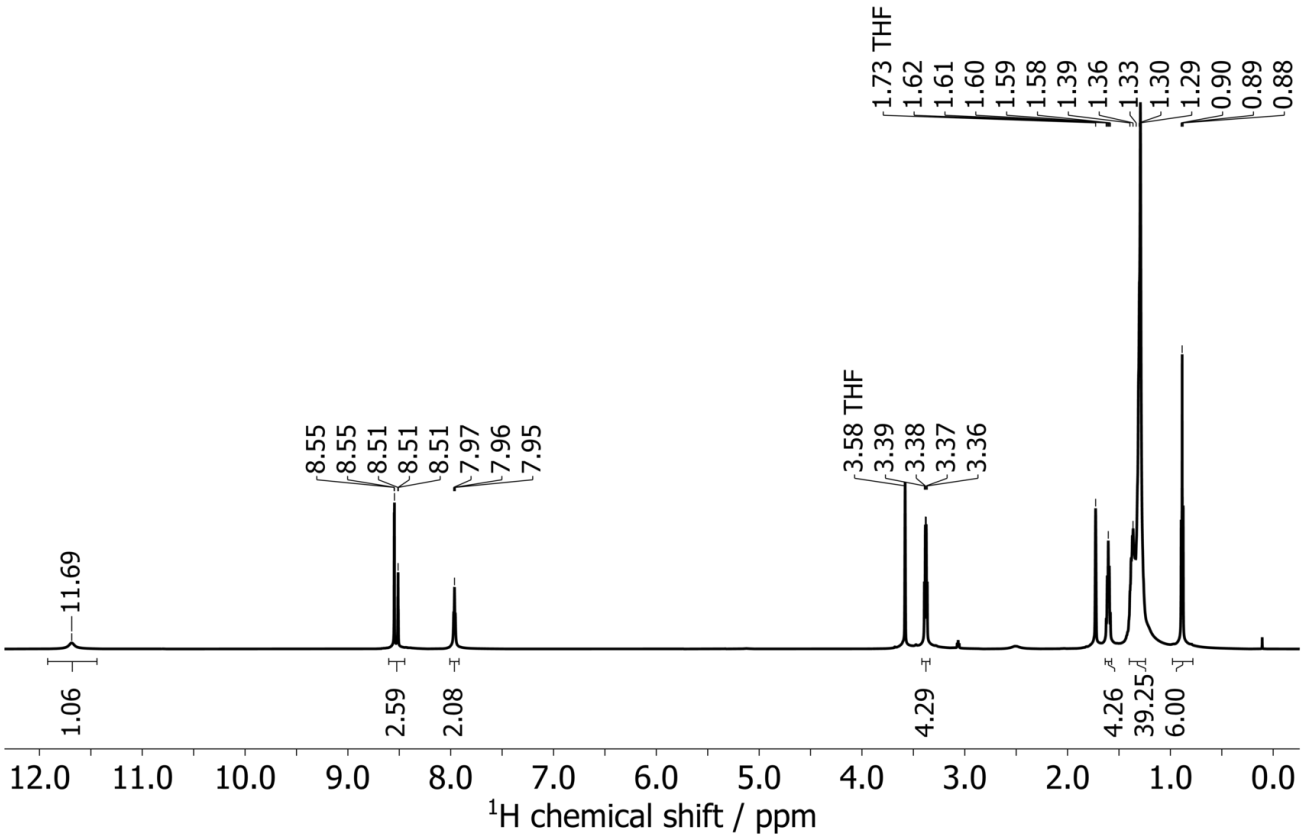

^{13}C-NMR

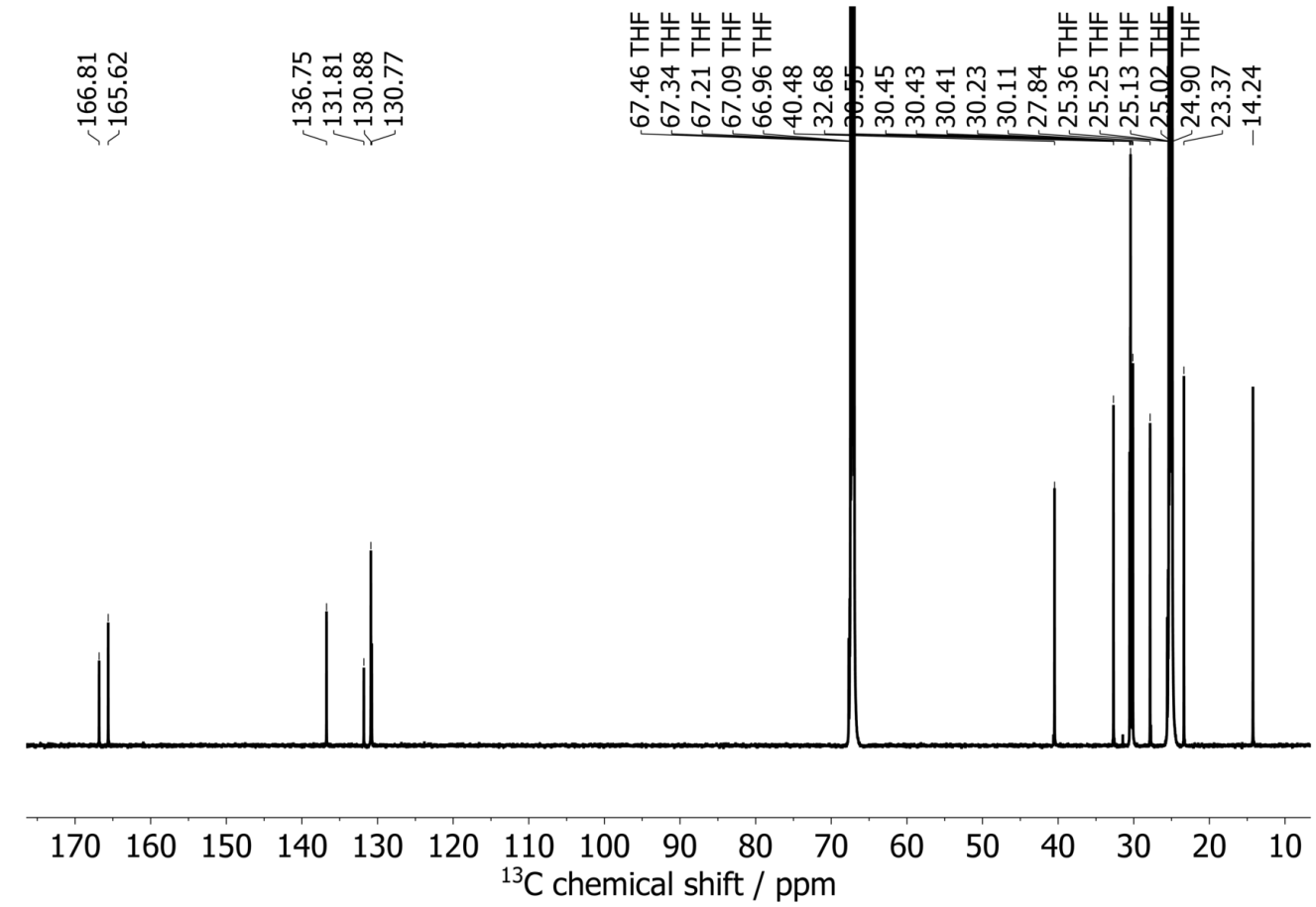

HRMS(ESI^{+})

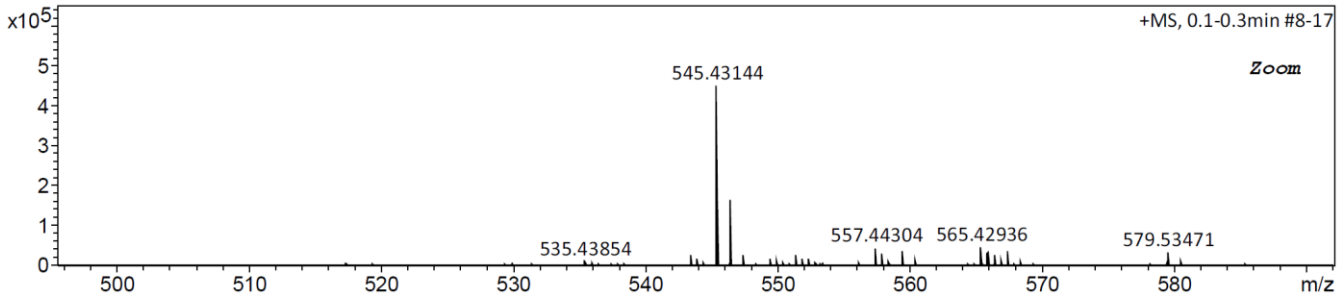

S4.4 (*R*)-*N*^{1},*N*^{3}-didodecyl-*N*^{5}-(Octan-2-yl)benzene-1,3,5-tricarboxamide (*R*)-2

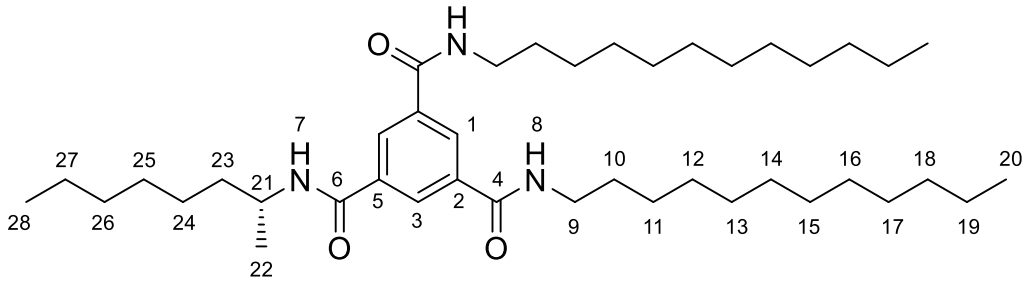

Synthesis of (*R*)-N^1,N^3-didodecyl-N^5-(octan-2-yl)benzene-1,3,5-tricarboxamide (*R*)-**2:**

(*R*)-**2** was prepared by dissolving 3,5-bis(dodecyl-carbamoyl)benzoic acid **10** (1.864 g, 3.42 mmol, 1.0 eq.) under argon atmosphere in 40 mL dried THF. The solution was cooled to 0 °C and 1,1'-Carbonyldiimidazole **8** (0.582 g, 3.59 mmol, 1.05 eq. was added. After the solution was stirred for 22 h at room temperature, (*R*)-octan-2-amine **11** (0.476 g, 3.59 mmol, 1.05 eq.) with 20 mL dried THF was added dropwise at 0 °C and the solution was stirred for another 48 h at room temperature. After removal of the solvent under vacuum 2.851 g of the crude product were suspended in 130 mL dichloromethane and washed with 50 mL 1 M hydrochloric acid and saturated solutions of sodium chloride and bicarbonate. After removal of the solvent the product (2.124 g, 94.6 %) was obtained by purification via column chromatography eluting with $CHCl_3$/EtOAc (4:15) as a colorless solid.
R_f = 0.38 (petroleum ether/EtOAc 1:1);

^{1}H-NMR (700 MHz, 300 K, [D_8]THF): δ=8.38 (s, 3-$H_{1\&3}$), 7.99 (t, 2-N-H_8, J = 5.11 Hz), 7.69 (d, 1-N-H_7, J = 8.08 Hz), 4.16 (m, 1-H_{21}), 3.37 (m, 4-H_9), 1.60 (m, 5-$H_{10\&23}$), 1.50 (m, 1-H_{23}), 1.40 – 1.25 (m, 47-$H_{11\text{-}19\&24\text{-}27}$, calc. 44, found 47), 1.20 (d, 3-H_{22}, ^{3}J = 6.65 Hz), 0.89 (m, 9-$H_{20\&28}$) ppm ^{13}C-NMR (175 MHz, 300 K, [D_8]THF): δ=166.08 (C_4), 165.61 (C_6), 136.62 (C_5), 136.36 (C_2), 128.67 (C_3), 128.58 (C_1), 46.14 (C_{21}), 40.46 (C_9), 37.45 (C_{23}), 30.58 (C_{10}), 27.85 (C_{11}), 27.13 (C_{24}), 32.69, 32.64, 30.46 – 30.41, 30.25, 30.12, 30.08 23.37, 23.36 ($C_{12\text{-}19\&25\text{-}27}$), 21.04 ($C_{22}$), 14.25 ($C_{20\&28}$) ppm; HRMS (ESI): m/z calc. for $C_{41}H_{73}N_3O_3$+H^+: 656.5725 [M+H]$^+$; found: 656.5726; [α]D20=14 (β=1.15·10^{-3} g/mL in DMSO);

^{1}H-NMR

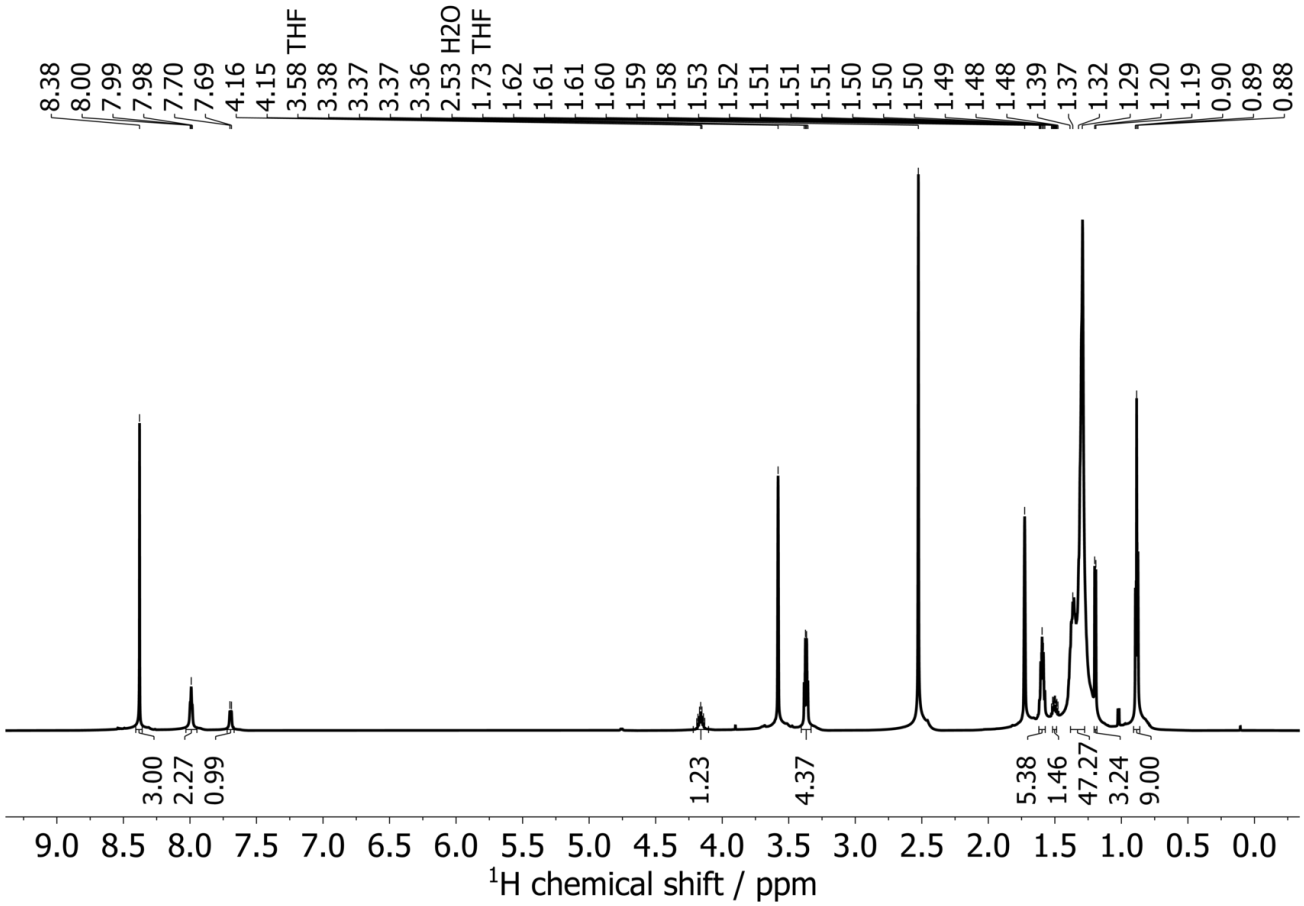

^{13}C-NMR

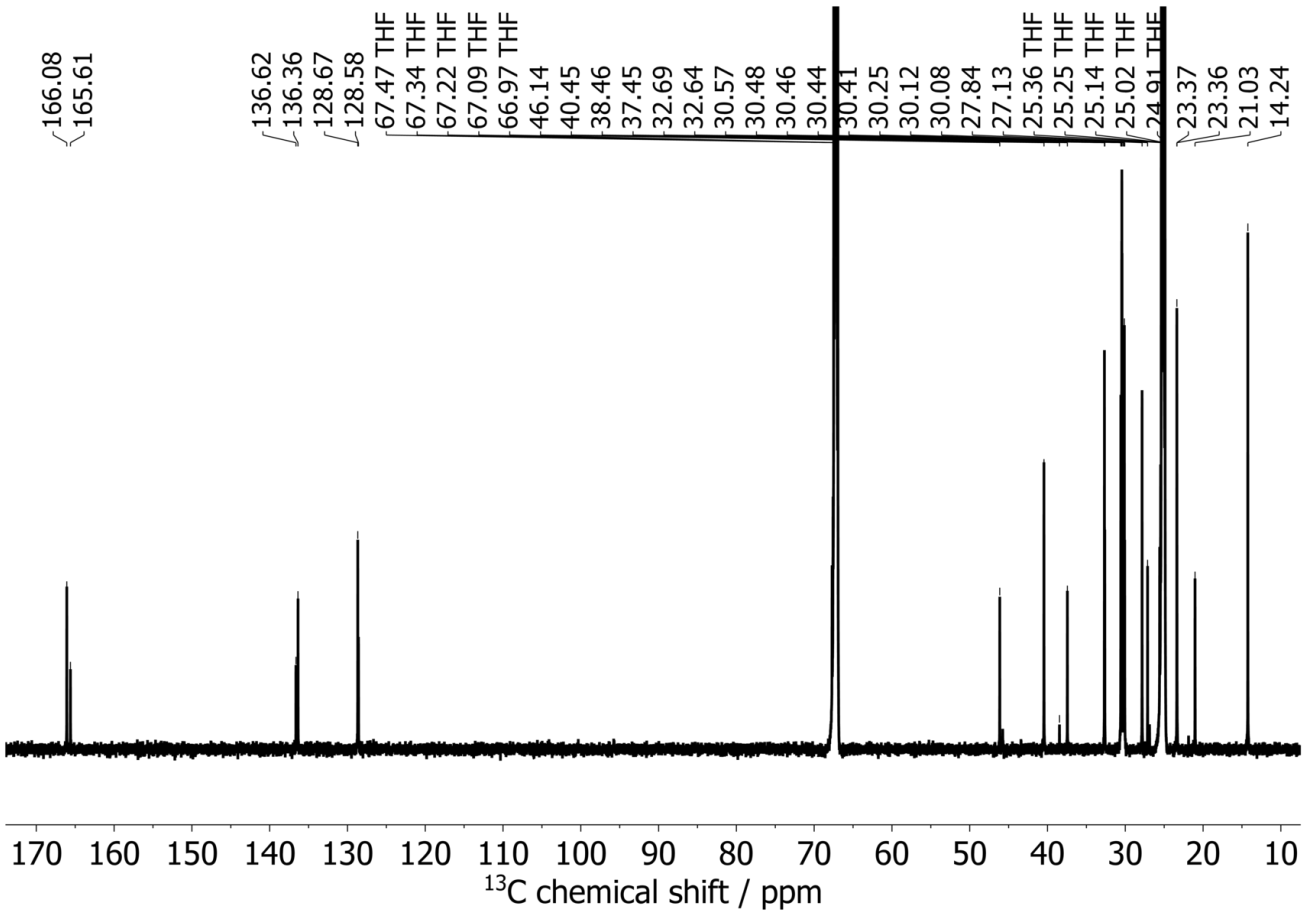

HRMS(APCI^{+})

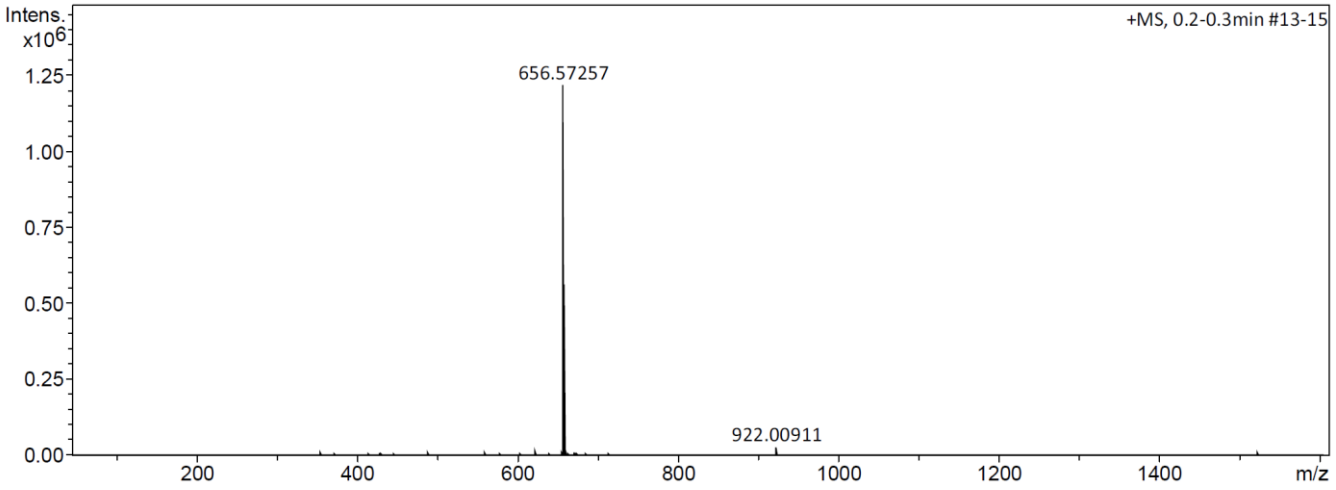

S4.5 (*S*)-*N*^{1},*N*^{3}-didodecyl-*N*^{5}-(Octan-2-yl)benzene-1,3,5-tricarboxamide (*S*)-2

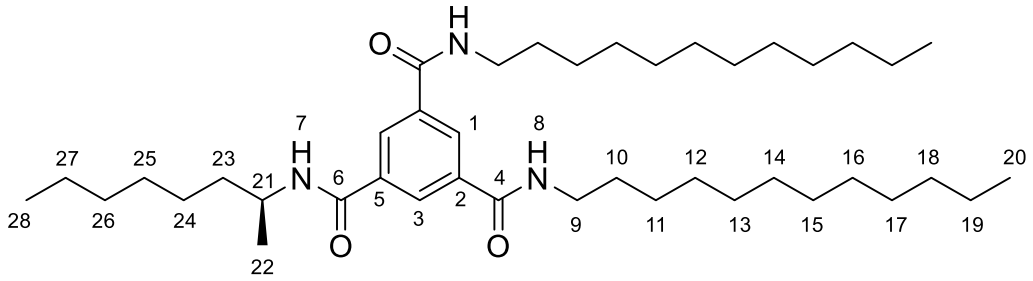

Synthesis of (*S*)-N^1,N^3-didodecyl-N^5-(octan-2-yl)benzene-1,3,5-tricarboxamide (*S*)-**2:**

The enantiomeric (*S*)-N^1,N^3-didodecyl-N^5-(octan-2-yl)benzene-1,3,5-tricarboxamide (*S*)-**2** was synthesized analogues according to the procedure described for the R enantiomer (*R*)-**2** above using (*S*)-octan-2-amine **12**. The product was obtained as a colorless solid (77.2 %).
R_f = 0.51 (petroleum ether/EtOAc 1:1);

^{1}H-NMR (400 MHz, 300 K, [D_8]THF): δ=8.38 (s, 3-$H_{1\&3}$), 8.00 (t, 2-N-H_8, J = 5.61 Hz), 7,71 (d, 1-N-H_7, J = 8.27 Hz), 4.16 (m, 1-H_{21}), 3.37 (m, 4-H_9), 1.59 (m, 5-$H_{10\&23}$), 1.50 (m, 1-H_{23}), 1.40 – 1.25 (m, 48-$H_{11\text{-}19\&24\text{-}27}$; calc. 44, found 48), 1.19 (d, 3-H_{22}, ^{3}J = 6.66 Hz), 0.89 (m,6-H_{20}), 0.88 (m, 3-H_{28}) ppm ^{13}C-NMR (100 MHz, 300 K, [D_8]THF): δ=166.09 (C_4), 165.63 (C_6), 136.62 (C_5), 136.35 (C_2), 128.68 (C_3), 128.59 (C_1), 46.13 (C_{21}), 40.46 (C_9), 37.44 (C_{23}), 30.56 (C_{10}), 27.84 (C_{11}); 27.13 (C_{24}), 32.68, 32.62, 30.45 – 30.41, 30.24, 30.11, 30.07 23.37 ($C_{12\text{-}19\&25\text{-}27}$), 21.03 ($C_{22}$), 14.24 ($C_{20\&28}$) ppm. HRMS (ESI): m/z calc. for $C_{41}H_{73}N_3O_3$+H^+: 656.5725 $[M+H]^+$; found: 656.5729; [α]D20=-14 (β=1.18·10^{-3} g/mL in DMSO);

^{1}H-NMR

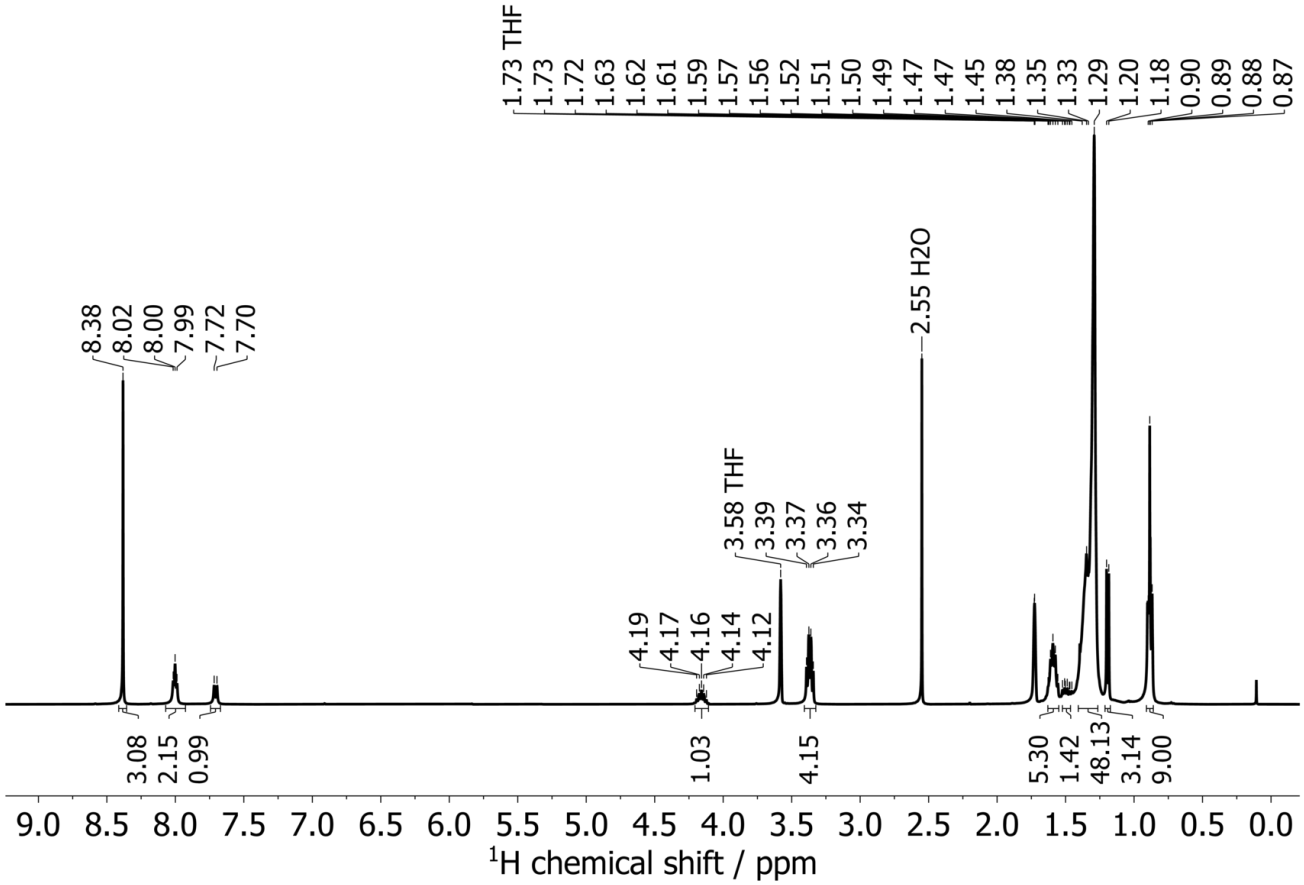

^{13}C-NMR

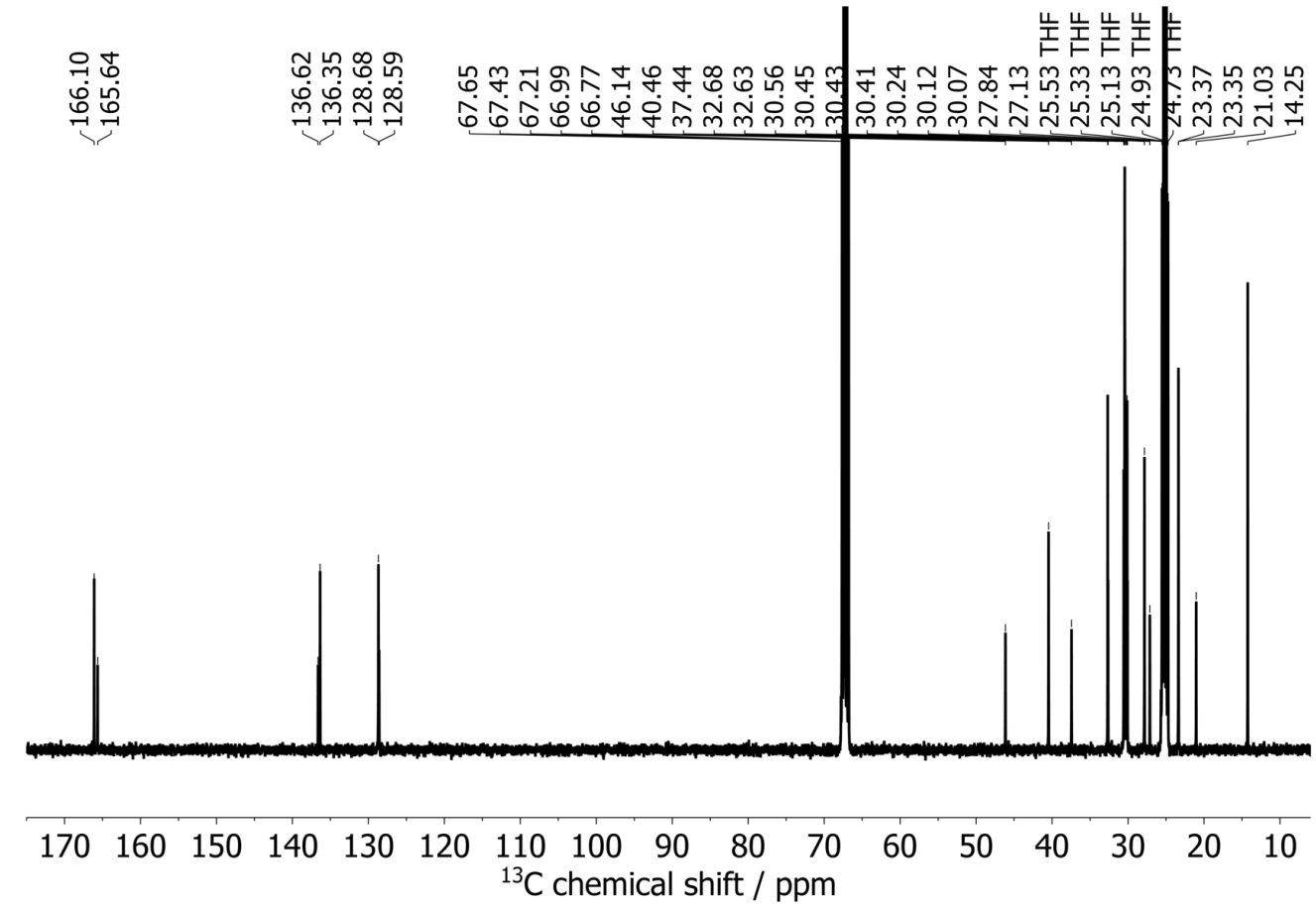

HRMS(APCI^{+})

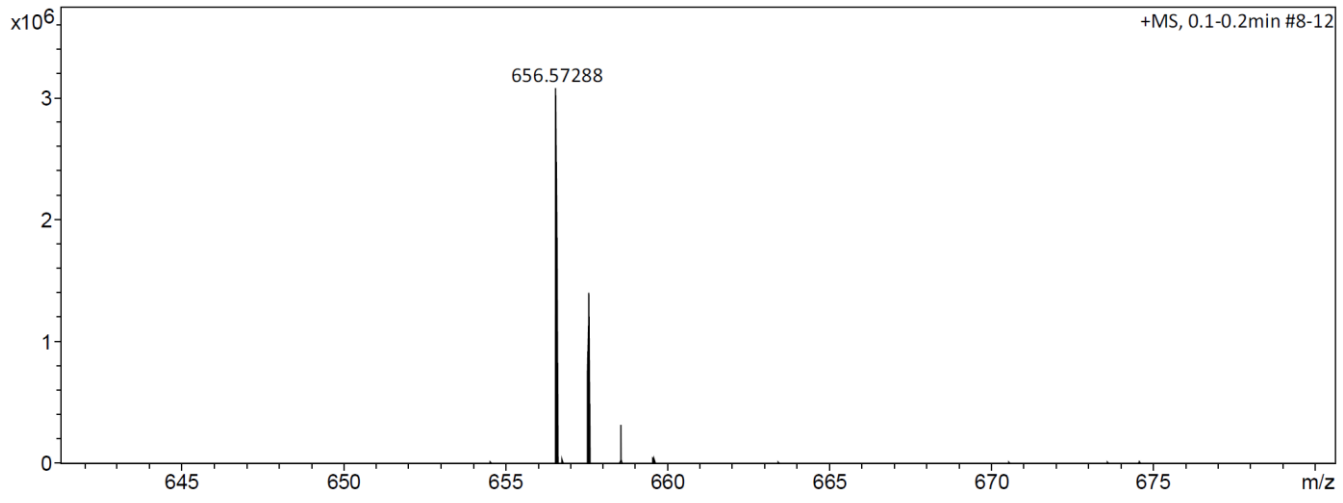

SUPPORTING INFORMATION

S5. References

[1] M. Leyendecker, N.-C. Meyer, C. M. Thiele, *Angew. Chem. Int. Ed.* **2017**, *56*, 11471-11474.
[2] P. Trigo-Mouriño, C. Merle, M. R. M. Koos, B. Luy, R. R. Gil, *Chem. Eur. J.* **2013**, *19*, 7013-7019.
[3] a) A. Enthart, J. C. Freudenberger, J. Furrer, H. Kessler, B. Luy, *J. Magn. Reson.* **2008**, *192*, 314-322; b) L. Castañar, E. Sistaré, A. Virgili, R. T. Williamson, T. Parella, *Magn. Reson. Chem.* **2015**, *53*, 115-119.
[4] a) D. Sinnaeve, M. Foroozandeh, M. Nilsson, G. A. Morris, *Angew. Chem. Int. Ed.* **2016**, *55*, 1090-1093; b) D. Sinnaeve, J. Ilgen, M. E. Di Pietro, J. J. Primozic, V. Schmidts, C. M. Thiele, B. Luy, *Angew. Chem.* **2020**, *132*, 5354-5358.
[5] E. Kupce, J. Boyd, I. D. Campbell, *J. Magn. Reson. B* **1995**, *106*, 300-303.
[6] J. Saurí, P. Nolis, L. Castañar, A. Virgili, T. Parella, *J. Magn. Reson.* **2012**, *224*, 101-106.
[7] J. A. Aguilar, M. Nilsson, G. Bodenhausen, G. A. Morris, *Chem. Commun.* **2012**, *48*, 811-813.
[8] M. Foroozandeh, R. Adams, P. Kiraly, M. Nilsson, G. Morris, *Chem. Commun.* **2015**, *51*, 15410-15413.
[9] L. Verdier, P. Sakhaii, M. Zweckstetter, C. Griesinger, *J. Magn. Reson.* **2003**, *163*, 353-359.
[10] M. Alcaraz Janssen, C. M. Thiele, *Chem. Eur. J.* **2020**, *26*, 7831-7839.
[11] G. Kummerlowe, S. Schmitt, B. Luy, *Open. Spectrosc. J.* **2010**, *4*.
[12] a) R. Berger, C. Fischer, M. Klessinger, *J. Phys. Chem. A* **1998**, *102*, 7157-7167; b) V. Schmidts, Technische Universität (Darmstadt), **2013**.
[13] a) J. W. Tukey, *Ann. Math. Statist.* **1958**, *29*, 614-623; b) C. M. Thiele, V. Schmidts, B. Böttcher, I. Louzao, R. Berger, A. Maliniak, B. Stevensson, *Angew. Chem. Int. Ed.* **2009**, *48*, 6708-6712.
[14] G. Cornilescu, J. L. Marquardt, M. Ottiger, A. Bax, *J. Am. Chem. Soc.* **1998**, *120*, 6836-6837.
[15] J. A. Losonczi, M. Andrec, M. W. Fischer, J. H. Prestegard, *Vol. 138*, Academic Press, **1999**, pp. 334-342.
[16] a) C. Lee, W. Yang, R. G. Parr, *Phys. Rev. B* **1988**, *37*, 785-789; b) A. D. Becke, *J. Chem. Phys.* **1993**, *98*, 5648-5652.
[17] a) F. Weigend, R. Ahlrichs, *Phys. Chem. Chem. Phys.* **2005**, *7*, 3297-3305; b) F. Weigend, *Phys. Chem. Chem. Phys.* **2006**, *8*, 1057-1065.
[18] a) F. Neese, *Wiley Interdiscip. Rev. Comput. Mol. Sci.* **2018**, *8*, e1327; b) F. Neese, *Wiley Interdiscip. Rev. Comput. Mol. Sci.* **2022**, *12*, e1606.